Optimal control of sweeping processes in unmanned surface vehicle and nanoparticle modelling

Boris S. Mordukhovich, Dao Nguyen, and Trang Nguyen

QUERY SHEET

This page lists questions we have about your paper. The numbers displayed at left are hyperlinked to the location of the query in your paper.

The title and author names are listed on this sheet as they will be published, both on your paper and on the Table of Contents. Please review and ensure the information is correct and advise us if any changes need to be made. In addition, please review your paper as a whole for typographical and essential corrections.

Your PDF proof has been enabled so that you can comment on the proof directly using Adobe Acrobat. For further information on marking corrections using Acrobat, please visit https://authorservices.taylorandfrancis.com/how-to-correct-proofs-with-adobe/

The CrossRef database (www.crossref.org/) has been used to validate the references.

AUTHOR QUERIES

QUERY NO.	QUERY DETAILS
Q1	Please note that the journal allows a maximum of '5' keywords. Please edit keywords accordingly.
Q2	The disclosure statement has been inserted. Please correct if this is inaccurate.
Q3	The CrossRef database (www.crossref.org/) has been used to validate the references. Mismatches between the original manuscript and CrossRef are tracked in red font. Please provide a revision if the change is incorrect. Do not comment on correct changes.

2

4

5

6 7

8 9

10

11 12

13

14

15

16

17

18

19

20

21

22

23

24

252627

28

29 30

31

32 33

34

35 36

37

38

39

40 41

42

43





Optimal control of sweeping processes in unmanned surface vehicle and nanoparticle modelling

Boris S. Mordukhovich^a, Dao Nguyen^b and Trang Nguyen^a

^aDepartment of Mathematics, Wayne State University, Detroit, MI, USA; ^bDepartment of Mathematics and Statistics, San Diego State University, San Diego, CA, USA

ABSTRACT

This paper addresses novel applications to practical modelling of the newly developed theory of necessary optimality conditions in controlled sweeping/Moreau processes with free time and pointwise control and state constraints. Problems of this type appear, in particular, in dynamical models dealing with unmanned surface vehicles (USVs) and nanoparticles. We formulate optimal control problems for a general class of such dynamical systems and show that the developed necessary optimality conditions for constrained free-time controlled sweeping processes lead us to designing efficient procedures to solve practical models of this class. Moreover, the paper contains numerical calculations of optimal solutions to marine USVs and nanoparticle models in specific situations. Overall, this study contributes to the advancement of optimal control theory for constrained sweeping processes and its practical applications in the fields of marine USVs and nanoparticle modelling.

ARTICLE HISTORY

Received 21 November 2023 Accepted 25 May 2024

KEYWORDS

Sweeping processes; optimal control; marine surface vehicles; nanoparticles; variational analysis; necessary optimality conditions; discrete approximations; generalized differentiation

Q1

2020 MATHEMATICS SUBJECT CLASSIFICATIONS

49J52; 49J53; 49K24; 49M25; 90C30

1. Introduction

Sweeping process models, initially termed 'processus de rafle', were pioneered by Jean-Jacques Moreau in the 1970s as a means to elucidate the dynamics inherent in elastoplasticity and related mechanical domains; see, e.g. [1]. Such models, described in the form of the dissipative differential inclusions of the type

$$\begin{cases} \dot{x}(t) \in -N(x(t); C(t)) \text{ a.e. } t \in [0, T], \\ x(0) = x_0 \in C(0) \subset \mathbb{R}^n, \end{cases}$$
 (1)

via the normal cone to the convex moving sets C(t), have been expounded upon in many publications by Moreau and other researchers. We list here just a few of them [2–15], where the reader can find further references to theoretical developments and various applications to aerospace, process control, robotics,

CONTACT Boris S. Mordukhovich boris@math.wayne.edu Dedicated to Lionel Thibault, with deep respect and admiration

45

46

47 48

49

50 51

52 53

54 55

56

57 58

59

60

61 62

63

64

65

66

67 68

69

70

71

72 73

74

75

76

77 78

79 80

81

82 83 bioengineering, chemistry, biology, economics, finance, management science, and engineering.

Lionel Thibault, a colleague of Moreau, has made fundamental contributions to the theory of sweeping processes in finite and infinite dimensions; see, e.g. [2, 13, 16, 17] and the references therein.

Since the Cauchy problem for sweeping processes of type (1) admits a *unique* solution under natural assumptions, there is no room for optimization in the framework of (1). More recently, some optimization problems have been formulated and investigated for various controlled sweeping processes, where control actions enter moving sets, adjacent differential equations, and/or perturbations of the sweeping dynamics. We refer the reader to the stream of rather recent publications [18–32] and the bibliographies therein, where *necessary optimality* conditions have been established and applied to models of friction and plasticity, robotics, traffic equilibria, ferromagnetism, hysteresis, and other fields of applied sciences.

It should be mentioned that deriving necessary optimality conditions for controlled sweeping problems is much more challenging in comparison with optimal control of ODEs and Lipschitzian differential inclusions of the type $\dot{x} \in F(x)$; see, e.g. [33-35]. The main difficulties come from the intrinsic discontinuity of the sweeping dynamics described by the normal cone mappings and the intrinsic presence of pointwise state as well as irregular mixed constraints on control and state functions.

This paper is devoted to applications of the novel theory of necessary optimality conditions developed in [36] for a new class of controlled sweeping processes with free time and hard control-state constraints. For the first time in the literature, we address here practical optimal control models, which naturally arise in the dynamical modelling of marine unmanned surface vehicles and nanoparticles. In fact, the theoretical developments in [36] have been largely motivated by the applications presented in this paper.

In Section 2, we formulate and discuss the free-time sweeping optimal control problem of our study with overviewing some major results on discrete approximations and necessary optimality conditions distilled from [36]. Employing these developments, we consider in Section 3 a broad class of planar dynamical models, which can be delineated via the free-time sweeping optimal control problem investigated in Section 2. Sections 4 and 5 formulate and study in detail optimal control problems for marine USVs and nanoparticles, respectively, with calculating optimal solutions to these models by using the obtained necessary optimality conditions for controlled sweeping constrained systems. The concluding Section 6 summarizes the underlying features of the developed models and obtained results with discussing some directions of the future research.

2. Sweeping optimal control with free time

First we formulate a general free-time optimal control problem for the sweeping dynamics and highlight (with additional discussions and comments) some pivotal findings from [36] that are essential for the subsequent applications to practical modelling. By (P), we label the sweeping optimal control problem described as follows:

minimize
$$J[x, u, T] := \varphi(x(T), T)$$

over measurable controls $u(\cdot)$ and absolutely continuous sweeping trajectories $x(\cdot)$ defined on the variable time interval [0, T] and satisfying the dynamic, control, and endpoint constraints

$$\begin{cases} \dot{x}(t) \in -N\left(x(t); C(t)\right) + g\left(x(t), u(t)\right) \text{ a.e. } t \in [0, T], \ x(0) \\ = x_0 \in C(0) \subset \mathbb{R}^n, \\ u(t) \in U \subset \mathbb{R}^d \text{ a.e. } t \in [0, T], \\ (x(T), T) \in \Omega_x \times \Omega_T \subset \mathbb{R}^n \times [0, \in fty), \end{cases}$$

$$(2)$$

where Ω_x and Ω_T are subsets of \mathbb{R}^n and $[0, \in fty)$, respectively, and where C(t) is a convex polyhedron given by

$$\begin{cases}
C(t) := \bigcap_{j=1}^{s} C^{j}(t) \text{ with } C^{j}(t) := \left\{ x \in \mathbb{R}^{n} \mid \langle x_{*}^{j}(t), x \rangle \leq c_{j}(t) \right\}, \\
\|x_{*}^{j}(t)\| = 1, j = 1, \dots, s, t \in [0, \in fty).
\end{cases}$$
(3)

Recall that the normal cone to the convex set in (2) is defined by

$$N(x;C) := \left\{ v \in \mathbb{R}^n \mid \langle v, y - x \rangle \le 0, \ y \in C \right\} \quad \text{if } x \in C \quad \text{and}$$

$$N(x;C) := \emptyset \text{ if } x \notin C.$$

The latter tells us that problem (P) automatically contains the pointwise state constraints

$$x(t) \in C(t)$$
, i.e. $\langle x_*^j(t), x(t) \rangle \leq c_j(t)$ for all $t \in [0, T]$ (with different T) and $j = 1, \dots, s$.

In fact, the sweeping dynamics intrinsically induce irregular mixed constraints on controls and trajectories that are the most challenging and largely underinvestigated even in classical control theory for smooth ODEs.

All the triples $(x(\cdot), u(\cdot), T) \in W^{1,2}([0, T]; \mathbb{R}^n) \times L^2([0, T]; \mathbb{R}^d) \times \mathbb{R}_+$ satisfying (2) are called *feasible solutions* to (P). We identify the trajectory $x:[0,T] \rightarrow$

$$x_e(t) := x(T) \quad \text{for all } t > T,$$

and for $x(\cdot) \in W^{1,2}([0,T],\mathbb{R}^n)$ define the norm

$$||x||_{W^{1,2}} := ||x(0)|| + ||\dot{x}_e||_{L_2}.$$

Let us now specify what we mean by a $W^{1,2} \times L^2 \times \mathbb{R}_+$ -local minimizer for (P) and its relaxation; cf. [26] when the duration of the process is fixed.

Definition 2.1: A feasible solution $(\bar{x}(\cdot), \bar{u}(\cdot), \overline{T})$ to problem (P) qualifies as a $W^{1,2} \times L^2 \times \mathbb{R}_+$ -local minimizer for this problem if there exists $\epsilon > 0$ such that $J[\bar{x}, \bar{u}, \overline{T}] \leq J[x, u, T]$ holds for all feasible solutions $(x(\cdot), u(\cdot), T)$ to (P) satisfying the localization condition

$$\in t_0^{\overline{T}} \left(\left\| \dot{x}_e(t) - \dot{\overline{x}}_e(t) \right\|^2 + \left\| u(t) - \overline{u}(t) \right\|^2 \right) dt + (\overline{T} - T)^2 < \epsilon.$$

The *relaxed* version (*R*) of problem (*P*) is constructed as follows:

minimize
$$\widehat{J}[x, u, T] := \varphi(x(T), T)$$

over absolutely continuous trajectories of the convexified differential inclusion

$$\dot{x}(t) \in -N(x(t); C(t)) + \cos g(x(t), U)$$

a.e. $t \in [0, T], x(0) = x_0 \in C(t) \subset \mathbb{R}^n,$ (4)

where 'co' represents the convex hull of the set.

Definition 2.2: Let $(\bar{x}(\cdot), \bar{u}(\cdot), \bar{T})$ be a feasible solutions for problem (P). We say that it is a relaxed $W^{1,2} \times L^2 \times \mathbb{R}_+$ -local minimizer for (P) if the following condition holds: there exists $\epsilon > 0$ such that

$$\varphi\left(\bar{x}(\cdot), \overline{T}\right) \le \varphi\left(x(\cdot), T\right) \quad \text{whenever}$$

$$\in t_0^{\overline{T}} \left(\left\|\dot{x}_e(t) - \dot{\bar{x}}_e(t)\right\|^2 + \left\|u(t) - \bar{u}(t)\right\|^2 \right) dt + (\overline{T} - T)^2 < \epsilon,$$

where $u(t) \in \text{co } U$ a.e. on [0, T] with $u(\cdot)$ representing a measurable control, and $x(\cdot)$ denotes a relaxed trajectory of the convexified inclusion (4), which can be uniformly approximated in $W^{1,2}([0, T]; \mathbb{R}^n)$, by feasible trajectories to (P) generated by piecewise constant controls $u^k(\cdot)$ on [0, T], the convex combinations of which converge strongly to $u(\cdot)$ in the norm topology $L^2([0, T]; \mathbb{R}^d)$.

It follows from the construction of the relaxed problem (R) that the local minimizers in Definitions 2.1 and 2.2 agree under the convexity assumptions on the data of (P). Due to the nonatomicity of the Lebesgue measure, such a relaxation

stability phenomenon also holds in broad nonconvex settings; see [26, 36] for more details.

Now we formulate the standing assumptions on the given data of the sweeping control system in (2) and (3), which are all satisfied in the practical models studied in the subsequent sections.

178 179

180

181

182 183

184

185

190

191 192

193 194

195

196

197

198

199 200 201

202

203 204

205 206

207

208

209

210 211

212

213

214 215

173

174

175 176

177

- (H1) The control set $U \neq \emptyset$ is closed and bounded in \mathbb{R}^d .
- (H2) The generating functions $x_*^{j}(\cdot)$ and $c_i(\cdot)$ of the moving polyhedron in (3) are Lipschitz continuous with a common Lipschitz constant *L*.
- (H3) The uniform Slater condition is fulfilled:

for every
$$t \in [0, T]$$
 there exists $x \in \mathbb{R}^n$ such that $\langle x_*^j(t), x \rangle$
 $\langle c_i(t) \text{ whenever } i = 1, \dots, s.$ (5)

186 (H4) The perturbation mapping $g: \mathbb{R}^n \times U \to \mathbb{R}^n$ exhibits *Lipschitz continuity* 187 with respect to x uniformly on U whenever x belongs to a bounded subset 188 of \mathbb{R}^n , and the sublinear growth condition holds: there is $\beta > 0$ with 189

$$||g(x, u)|| \le \beta (1 + ||x||)$$
 for all $u \in U$.

(H5) The endpoint-final time constraint set $\Omega_x \times \Omega_T$ is closed.

Note that the uniform Slater condition (5), introduced recently in [29] always holds under the fulfilment of the linear independence constraint qualification (LICO)

$$\left[\sum_{j\in I(t,x)} \lambda_j x_*^j(t) = 0, \quad \lambda_j \in \mathbb{R}\right] \Longrightarrow \left[\lambda_j = 0 \text{ for all } j \in I(t,x)\right], \tag{6}$$

where the moving active index set at (t, x) is defined by

$$I(t,x) := \left\{ j \in \{1,\ldots,s\} \mid \langle x_*^j(t), x \rangle = c_j(t) \right\}.$$

On the other hand, (5) yields the positive linear independence constraint qualification (PLICQ) corresponding to (6) with $\lambda_i \in \mathbb{R}$ replaced by $\lambda_i \in \mathbb{R}_+$ for $j \in I(t, x)$. It follows from [29, Theorem 2] that the assumptions imposed above ensure that any feasible control $u(\cdot)$ to (P) generates the unique Lipschitz continuous trajectory $x(\cdot)$ of the sweeping process in (2).

Our approach to the study and solving dynamic optimization problems is based on the method of discrete approximations developed by the first author [34, 37] for Lipschitzian differential inclusions. Since the sweeping dynamics is highly non-Lipschitzian, applications of this method to controlled sweeping processes require significant modifications, which have been done in [21, 24, 26, 36, 38–41] for various classes of sweeping control problems. To proceed in the setting of (2)

$$t_0^k = 0$$
, $t_{i+1}^k = t_i^k + h^k$ as $i = 0, 1, \dots, k-1$, $t_k^k := T_k$, $h^k := k^{-1}T_k$. (7)

The following result, distilled from [36, Theorem 2.3], verifies a *strong approximation* of *any feasible solution* to the continuous-time sweeping control problem (*P*) by a sequence of feasible solutions to perturbed *discrete-time sweeping processes*. Beside being useful in deriving necessary optimality conditions for (*P*), this result justifies the possibility to replace the infinite-dimensional sweeping dynamics by its finite-dimensional counterparts in *numerical calculations*, which is important for practical modelling.

Theorem 2.3: Let $(\bar{x}(\cdot), \bar{u}(\cdot), \bar{T}) \in W^{1,2}([0, \bar{T}]; \mathbb{R}^n) \times L^2([0, \bar{T}]; \mathbb{R}^d)$ be an arbitrary feasible solution to problem (P) under the imposed standing assumptions. Then we have the assertions:

(i) There exists a sequence of piecewise constant functions $\{u^k(\cdot) \mid k \in N\}$ such that $u^k(\cdot) \to \bar{u}(\cdot)$ strongly in the L^2 -norm topology on $[0, \overline{T}]$ as $k \to \in fty$.

(ii) There exists a sequence of piecewise linear functions $\{x^k(\cdot) \mid k \in N\}$, which converges strongly to $\bar{x}(\cdot)$ in the $W^{1,2}$ -norm topology on $[0, \overline{T}]$ with $x^k(0) = \bar{x}(0)$ for all $k \in N$ and such that

$$\dot{x}^k(t) \in -N(x^k(t_i^k); C_i^k) + g(x^k(t_i^k), u^k(t_i^k)) + \tau_i^k B, \quad t \in [t_i^k, t_{i+1}^k),$$

for i = 0, ..., k-1, where $\tau_i^k \ge 0$, $h^k \sum_{i=1}^{k-1} \tau_i^k \to 0$ as $k \to \in fty$, B stands for the closed unit ball, and the perturbed polyhedra C_i^k are defined by

$$C_i^k := \bigcap_{j=1}^s C_{ij}^k \quad with \ C_{ij}^k := \left\{ x \in \mathbb{R}^n \mid \langle x, x_*^j(t_i^k) \rangle \le c_k^{ij} \right\}$$

with some vectors $x_*^j(t_i^k)$ and numbers c_k^{ij} . Furthermore, all the approximating arcs $x^k(\cdot)$ are Lipschitz continuous on $[0, \overline{T}]$ with the same Lipschitz constant as $\bar{x}(\cdot)$.

(iii) The piecewise linear extensions of $x_{*k}^{j}(t_{j}^{k})$ and c_{k}^{ij} on the continuous time interval $[0, \overline{T}]$ converge uniformly on $[0, \overline{T}]$ as $k \to \in fty$ to $c_{j}(t)$ and $x_{*}^{j}(t)$, respectively.

Having in hand the strong approximation results of Theorem 2.3 applied to the designated relaxed $W^{1,2} \times L^2 \times \mathbb{R}_+$ -local minimizer $(\bar{x}(\cdot), \bar{u}(\cdot), \bar{T})$ of (P), we construct the sequence of *discrete approximation problems* (P_k) with a varying grid whose *optimal solutions exists* (assuming that the cost function φ

is lower semicontinuous) and strongly converge in $W^{1,2} \times L^2 \times \mathbb{R}_+$ -norm to $\{\bar{x}(\cdot), \bar{u}(\cdot), \bar{T}\}\$. For each $k \in N$, define problem (P_k) as follows:

minimize
$$J_k[x^k, u^k, T_k] := \varphi(x_k^k, T_k) + (T_k - \overline{T})^2$$

 $+ \sum_{i=0}^{k-1} \in t_{t_i^k}^{t_{i+1}^k} \left(\left\| \frac{x_{i+1}^k - x_i^k}{h^k} - \dot{\bar{x}}(t) \right\|^2 + \left\| u_i^k - \bar{u}(t) \right\|^2 \right) dt$

over $(x^k, u^k, T_k) := (x_0^k, x_1^k, \dots, x_{k-1}^k, x_k^k, u_0^k, u_1^k, \dots, u_{k-1}^k, T_k)$ satisfying the constraints

$$x_{i+1}^{k} - x_{i}^{k} \in -h^{k} F_{i}^{k}(t_{i}^{k}, x_{i}^{k}, u_{i}^{k}) \quad \text{for } i = 0, \dots, k - 1,$$

$$x_{0}^{k} := x_{0} \in C(0),$$

$$(x_{k}^{k}, T_{k}) \in \Omega_{x}^{k} \times \Omega_{T}^{k} := (\Omega_{x} + \delta^{k} B) \times (\Omega_{T} + \delta^{k}),$$

$$\sum_{i=0}^{k-1} \in t_{i_{i}}^{k+1} \left(\left\| \frac{x_{i+1}^{k} - x_{i}^{k}}{h^{k}} - \dot{x}(t) \right\|^{2} + \left\| u_{i}^{k} - \bar{u}(t) \right\|^{2} \right) dt \leq \epsilon,$$

$$\left\| \frac{x_{i+1}^{k} - x_{i}^{k}}{h^{k}} \right\| \leq L + 1 \quad \text{for all } i = 0, \dots, k - 1,$$

$$u_{i}^{k} \in U \quad \text{for } i = 0, \dots, k - 1,$$

$$\left\| ((x_{i}^{k}, u_{i}^{k}) - (\bar{x}(t_{i}^{k}), \bar{u}(t_{i}^{k})) \right\| \leq \epsilon \quad \text{for } i = 0, \dots, k - 1,$$

$$\left\| T_{k} - \overline{T} \right\| \leq \epsilon$$

$$\langle x_{*}^{j}(t), x_{k}^{k} \rangle \leq c_{i}(t) \quad \text{for all } j = 1, \dots, s,$$

$$(8)$$

where the discrete velocity mappings F_i^k are given by

$$F_i^k(t_i^k, x_i^k, u_i^k) := N(x_i^k; C_i^k) - g(x_i^k, u_i^k) - \tau_i^k B,$$

where $\delta^k := \|\bar{x}(\overline{T}) - \widehat{x}^k(\overline{T})\|$ with the sequence $\{x^k(\overline{T})\}$ constructed in Theorem 2.3 for $\bar{x}(\cdot)$, where $\epsilon > 0$ is taken from Definition 2.2 for $\bar{x}(\cdot)$, and where L is the Lipschitz constant of $\bar{x}(\cdot)$ on $[0, \bar{T}]$.

Employing Theorem 2.3 and using the construction of problems (P_k) allow us to verify the strong $W^{1,2} \times L^2 \times \mathbb{R}_+$ convergence of the extended (as in Theorem 2.3) optimal solutions to the designated local minimizer $(\bar{x}(\cdot, \bar{u}(\cdot), \bar{T}))$ of (P). This means that optimal solutions to the discrete approximation problems (P_k) can be viewed as *suboptimal solutions* to the original sweeping control problem (P).

To derive further precise necessary optimality conditions for the given local minimizer in (*P*), we develop the following *two-step procedure*:

Step A: Obtain necessary conditions for optimal solutions to (P_k)

303

304 305 306

307

308

309

310

311

312 313

314

315

316

317

318 319

320

321

322

323

324

325 326

327

328 329

330

331

332

333

334 335

336

337

338

339 340

341

342 343 344

Step B: By passing to the limit in the necessary optimality conditions for (P_k) as $k \to \in fty$, establish necessary optimality conditions for the designated local minimizers $(\bar{x}(\cdot), \bar{u}(\cdot), \overline{T})$ in (P).

The goal of Step A is accomplished by reducing each problem (P_k) to a mathematical program with geometric and functional constraints and deriving necessary optimality conditions in the latter setting by employing appropriate tools of generalized differentiation in variational analysis. Major requirements to such tools to be useful for furnishing the limiting procedure in Step B include robustness with respect to small perturbations, comprehensive calculus rules of generalized differentiation, and the ability to deal with geometric constraints of the graphical type (8), which are crucial to reflect the sweeping dynamics. Note to this end that Clarke's constructions of generalized differentiation [33] are not suitable for these purposes, since his normal cone is too large for graphical sets associated with functions and mappings even in very simple situations as, e.g. for the graph of f(x) := |x|, where Clarke's normal cone at (0,0) is the entire plane \mathbb{R}^2 . On the other hand, the limiting generalized differential constructions, introduced by the first author and then developed in numerous publications (see, e.g. the books [17, 42–44] and the references therein), provide the desired variational machinery for passing to the limit in Step B and deriving in this way an adequate collection of necessary optimality conditions in the sweeping control problem (P) that are satisfactory for applications to the practical models considered below.

The underlying feature of the sweeping dynamics and its discrete approximations is their descriptions via the normal cone mapping, which accumulates first-order information about the process. Thus the adjoint systems in both discrete-time and continuous-time problems unavoidably require a dual-type generalized derivative (coderivative) of normal cone mappings that are formalized by the first author as the second-order subdifferential (or generalized Hessian). The explicit calculations of this second-order construction for set-valued mappings, which appear in the sweeping dynamics (2) and (8), play a crucial in the realization of the method of discrete approximations for optimal control of sweeping processes. The reader can find such calculations and related results in the aforementioned papers on sweeping optimal control with the references therein. A comprehensive theory of second-order subdifferentials with a wide spectrum of applications is presented in [45].

To formulate the major necessary optimality conditions for problem (P) proved in [36, Theorem 5.2] by using the method of discrete approximations, we need the following notion. Observe to this end that Motzkin's theorem of the alternative gives us the representation of the normal cone N(x(t); C(t)) as $\left\{ \sum_{j \in I(t,x)} \eta^j(t) x_*^j(t) \mid \eta^j(t) \ge 0 \right\}.$

Definition 2.4: Let $x(\cdot)$ be a solution to the controlled sweeping process (2), i.e.

345 346

$$-\dot{x}(t) = \sum_{i=1}^{s} \eta^{i}$$

$$-\dot{x}(t) = \sum_{j=1}^{s} \eta^{j}(t) x_{*}^{j}(t) - g(x(t), u(t)) \quad \text{for all } t \in [0, T),$$

349 350

351

352

353

354

355

where $\eta_i \in L^2([0,T];\mathbb{R}^+)$ and $\eta_i(t) = 0$ for a.e. t such that $i \notin I(t,x(t))$. We say that the normal cone to C(t) is active along $x(\cdot)$ on the set $E \subset [0, T]$ if for a.e. $t \in E$ and all $j \in I(t, x(t))$ it holds that $\eta_i(t) > 0$. Denoting by E_0 the largest subset of [0, T] where the normal cone to C(t) is active along $x(\cdot)$ (i.e. the union of the density points of E such that the normal cone to C(t) is active with respect to this set), we simply say that the normal cone is active along $x(\cdot)$ provided that $E_0 = [0, T].$

356 357 358

359

360

361

362

Note that the requirement that the normal cone is active along a trajectory of (2) distinguishes (2) from trajectories of the classical controlled ODE $\dot{x} =$ g(x, u) which satisfy the tangency condition $\langle g(x(t), u(t)), x_*^j(t) \rangle < 0$ for a.e. t such that $i \in I(t, x(t))$ and thus $x(t) \in C(t)$ for all $t \in E$. Observe also that the above requirement holds automatically when the set I(t, x(t)) is empty, i.e. when x(t) stays in the interior of C(t).

363 364 365

366

367

368

369

370

371

374 375 **Theorem 2.5** ([36]): Let $(\bar{x}(t), \bar{u}(t), \overline{T})$, $0 < t < \overline{T}$, be a relaxed $W^{1,2} \times L^2 \times L^2$ \mathbb{R}_+ -local minimizer to problem (P). In addition to the standing assumptions, suppose that LICQ holds along $\bar{x}(t)$, $t \in [0, T]$, and that φ is locally Lipschitzian around $(\bar{x}(\bar{T}), \bar{T})$. Then there exist a multiplier $\mu \geq 0$, a nonnegative vector measure $\gamma_{>}=(\gamma_{>}^{1},\ldots,\gamma_{>}^{s})\in C^{*}([0,\overline{T}];\mathbb{R}^{s})$, and a signed vector measure $\gamma_{0}=$ $(\gamma_0^1,\ldots,\gamma_0^s)\in C^*([0,\overline{T}];\mathbb{R}^s)$ together with adjoint arcs $p(\cdot)\in W^{1,2}([0,\overline{T}];\mathbb{R}^n)$ and $q(\cdot) \in BV([0, \overline{T}]; \mathbb{R}^n)$ such that the following conditions are fulfilled:

372 373

• The sweeping trajectory representation

376 377

$$-\dot{\bar{x}}(t) = \sum_{j=1}^{s} \eta^{j}(t) x_{*}^{j}(t) - g(\bar{x}(t), \bar{u}(t)) \quad \text{for a.e. } t \in [0, \overline{T}),$$
 (9)

378 379

where the functions $\eta^{j}(\cdot) \in L^{2}([0,\overline{T}]);\mathbb{R}_{+})$ are uniquely determined for a.e. $t \in$ $[0, \overline{T})$ by representation (9).

380 381

• The adjoint arc inclusion

382 383

$$\left(-\dot{p}(t),\psi(t)\right)\in co\,\partial\langle q(t),g\rangle\,(\bar{x}(t),\bar{u}(t))\quad\text{ for a.e. }t\in[0,\overline{T}],$$

384 385

where the limiting subdifferential is taken with respect to (x, u), where $\psi(\cdot) \in$ $L^2([0,\overline{T}];\mathbb{R}^d)$ satisfies the

386 387

$$\psi(t) \in coN(\bar{u}(t); U)$$
 for a.e. $t \in [0, \overline{T}]$,

where the right continuous representative of $q(\cdot)$ is given by

$$q(t) = p(t) - \in t_{(t,\overline{T}]} \sum_{j=1}^{s} d\gamma^{j}(\tau) x_{*}^{j}(\tau)$$

for a.e. $t \in [0, \overline{T}]$ except at most a countable subset, and where $\gamma := \gamma_{>} + \gamma_{0}$. Moreover, $p(\overline{T}) = q(\overline{T})$.

• The tangential maximization condition: if the limiting normal cone is generated as

$$N(\bar{u}(t); U) = T^*(\bar{u}(t); U) := \left\{ v \in \mathbb{R}^n \mid \langle v, u \rangle \le 0 \text{ for all } u \in T(\bar{u}(t); U) \right\}$$

by some tangent set $T(\bar{u}(t); U)$ associated with U at $\bar{u}(t)$, then we have

$$\langle \psi(t), \bar{u}(t) \rangle = \max_{u \in T(\bar{u}(t); U)} \langle \psi(t), u \rangle$$
 for a.e. $t \in [0, T]$.

In particular, the global maximization condition

$$\langle \psi(t), \overline{u}(t) \rangle = \max_{u \in U} \langle \psi(t), u \rangle$$
 for a.e. $t \in [0, \overline{T}]$

is satisfied provided that the control set *U* is convex.

• The dynamic complementary slackness conditions

$$\left\langle x_*^j(t), \bar{x}(t) \right\rangle < c_j(t) \Longrightarrow \eta^j(t) = 0 \quad and \quad \eta^j(t) > 0 \Longrightarrow \left\langle x_*^j(t), q(t) \right\rangle = 0$$

for a.e. $t \in [0, \overline{T}]$ and all indices j = 1, ..., s.

• The transversality conditions at the optimal final time: there exist numbers $\eta^j(\overline{T}) \geq 0$ whenever $j \in I(\overline{T}, \overline{x}(\overline{T}))$ ensuring the relationships

$$\left(-p(\overline{T}) - \sum_{j \in I(\overline{T}, \bar{x}(\overline{T}))} \eta^{j}(\overline{T}) x_{*}^{j}(\overline{T}), \bar{H}\right)$$

$$\in \mu \partial \varphi(\bar{x}(\overline{T}), \overline{T}) + N((\bar{x}(\overline{T}), \overline{T}); \Omega_{x} \times \Omega_{T}),$$

$$\eta^{j}(\overline{T}) > 0 \Longrightarrow j \in I(\overline{T}, \bar{x}(\overline{T})),$$
(10)

where $\overline{H} := \overline{T}^{-1} \in t_0^{\overline{T}} \langle p(t), \dot{\overline{x}}(t) \rangle dt$ is a characteristic of the optimal time.

• The endpoint complementary slackness conditions

$$\left\langle x_*^j(\overline{T}), \bar{x}(\overline{T}) \right\rangle < c_j(\overline{T}) \Longrightarrow \eta^j(\overline{T}) = 0 \quad \text{for all } j \in I\left(\overline{T}, \bar{x}(\overline{T})\right)$$

with the nonnegative numbers $\eta^{j}(\overline{T})$ taken from (10).

• The nonatomicity condition: If $t \in [0, \overline{T})$ and $\langle x_*^j(t), \overline{x}(t) \rangle < c_j$ for all $j = 1, \ldots, s$, then there exists a neighbourhood V_t of t in $[0, \overline{T})$ such that $\gamma_0^j(V) = 1$

 $\gamma_{>}^{j}(V) = 0$ for all Borel subsets V of V_{t} . In particular, supp $(\gamma_{>}^{j})$ and supp (γ_{0}^{j}) are contained in the set $\{t \mid i \in I(t, \bar{x}(t))\}.$

• The general nontriviality condition

$$(\mu, p, \|\gamma_0\|_{TV}, \|\gamma_0\|_{TV}) \neq 0,$$

accompanied by the support condition

$$\operatorname{supp}(\gamma_{>}) \cap \operatorname{int}(E_0) = \emptyset,$$

which holds provided the normal cone is active on a set with nonempty interior. • The enhanced nontriviality: we have $\mu = 1$ for the cost function multiplier in (10) provided that $\langle x_*^j(t), \bar{x}(t) \rangle < c_i(t)$ for all $t \in [0, \overline{T}]$ and all indices j = 1 $1, \ldots, s$.

In the subsequent sections, we develop applications of the obtained results to practical models formulated in the form of the sweeping optimal control problem (P).

3. Modeling

431 432

433

434

435 436

437 438

439

440

441

442

443 444

445

446

447 448 449

450

451

452

453

454

455

456

457

458

459

460

461

462

463

464 465

466

467

468 469

470

471

472

473

In this section, we delineate a class of rather general dynamical optimization models on the plane whose dynamics are described by sweeping processes. These models deal with n > 2 objects that have arbitrary shapes identified as virtual safety disks of different radius R_i , i = 1, ..., n, on the plane. Each object aims at reaching the target by the shortest path with the minimum time \overline{T} while avoiding the other n-1 static and/or dynamic obstacles. We define the configuration space of objects at some time $t \in [0, T]$ by the vector $x(t) = (x^1(t), \dots, x^n(t)) \in \mathbb{R}^{2n}$ with the variable ending time T, where $x^i(t) = (\|x^i(t)\| \cos \theta_i^x, \|x^i(t)\| \sin \theta_i^x) \in$ \mathbb{R}^2 denotes the Cartesian position of the *i*-th object, and where θ_i^x stands for the corresponding constant direction which is the smallest positive angle in standard position formed by the positive x-axis and vectors x^i with $0 \in \mathbb{R}^2$ as the target. The configuration is admissible when the motion of different objects is safe by imposing the noncollision/nonoverlapping condition. This can be formulated mathematically as

$$A := \{x = (x^1, \dots, x^n) \in \mathbb{R}^{2n} \mid D_{ij}(x) \ge 0 \text{ for all } i, j \in \{1, \dots, n\} \},$$

where $D_{ii}(x) := ||x^i - x^j|| - (R_i + R_i)$ is the distance between the disks i and j.

Describing the motion of objects without collisions can be outlined as follows: starting from an admissible configuration at time $t_k \in [0, T]$ (with different T), consider $x_k := x(t_k) \in A$. Then the next configuration after the period of time h > 0 is $x_{k+1} = x(t_k + h)$. To ensure a nonoverlapping motion of all objects at the next time $t_k + h$ for a small value of h > 0, the next configuration should also be admissible, i.e. $x(t_k + h) \in A$. This implies that the constraint $D_{ij}(x(t_k + h)) \ge 0$

should be satisfied. To verify the latter, by using the first-order Taylor expansion at $x_k \neq 0$ we deduce the constraint on the velocity vector as

 $D_{ii}(x(t_k + h)) = D_{ii}(x(t_k)) + h \nabla D_{ii}(x(t_k)) \dot{x}(t_k) + o(h),$ for small h > 0. (11)

where ∇D_{ii} is the gradient of the distance function. This constraint will be used to construct the next configuration or the next reference position of objects in order to avoid static and/or dynamic obstacles. In this regard, set the vector V(x)to be the desired velocity of all objects. The admissible velocities providing no collision during the navigation of objects are defined as

$$C_h(x) := \{ V(x) \in \mathbb{R}^{2n} \mid D_{ij}(x) + h \nabla D_{ij}(x) V(x) \ge 0 \text{ for all } i, j \in \{1, \dots, n\}, \ i < j \}, \ x \in \mathbb{R}^{2n}.$$

Taking now the admissible velocity $\dot{x}(t_k) \in C_h(x_k)$ gives us

$$D_{ij}(x_k) + h\langle \nabla D_{ij}(x_k), \dot{x}(t_k) \rangle \geq 0.$$

Skipping the term o(h) for small h, it follows from (11) that $D_{ii}(x(t_k + h)) \ge 0$, i.e. $x(t_k + h) \in A$. Since all the objects intend to reach the target by the shortest path, by taking into account that in the absence of obstacles the objects tend to keep their spontaneous velocities till reaching the target and that $||x^{i}(t)||$ $x^{j}(t) = R_{i} + R_{i}$ if the designated object touches the obstacles, we conclude that the object's velocity should be adjusted in order to keep the distance to be at least $R_i + R_i$ by using some *control actions* in the velocity term. The desired *controlled* velocities can be now represented as

$$g(x(t), u(t)) = (s_1 || u^1(t) || \cos \theta_1^u(t), s_1 || u^1(t) || \sin \theta_1^u(t), \dots, s_n || u^n(t) ||$$

$$\cos \theta_n^u(t), s_n || u^n(t) || \sin \theta_n^u(t)),$$

where θ_i^u stands for the corresponding constant direction, which is the smallest positive angle in standard position formed by the positive x-axis and vectors $u^i(t)$, and where $s_i \leq 0$ denotes the speed of the object i, with practically motivated control constraints represented by

$$u(t) = (u^{1}(t), \dots, u^{n}(t)) \in U \text{ for a.e. } t \in [0, T]$$
 (12)

with the control set $U \subset \mathbb{R}^n$ to be specified below in particular settings.

Having the above discussions in mind, let us describe the model dynamics as a sweeping process. To proceed, for any $k \in N$ consider the ending time T_k and the grid as in (7) with $x_i^k := x^k(t_i^k)$ for i = 1, ..., k. According to the model

description, we have the algorithm

 $x_0^k \in A$ and $x_{i+1}^k := x_i^k + h^k V_{i+1}^k$ for all i = 0, ..., k-1,

where V_{i+1}^k is defined as the *projection* of $g(x_i^k, u_i^k)$ onto the admissible velocity set $C_{hk}(x_i^k)$ by

$$V_{i+1}^k := \Pi\left(g(x_i^k, u_i^k); C_{h^k}(x_i^k)\right), \quad i = 0, \dots, k-1.$$
(13)

Using the construction of x_i^k for $0 \le i \le k-1$ and $k \in N$, design next a sequence of piecewise linear mappings $x^k \colon [0, T_k] \to \mathbb{R}^{2n}, k \in \mathbb{N}$, which pass through those points by

$$x^{k}(t) := x_{i}^{k} + (t - t_{i}^{k})V_{i+1}^{k} \quad \text{for all } t \in I_{i}^{k} := [t_{i}^{k}, t_{i+1}^{k})$$
(14)

with i = 0, ..., k - 1. Whenever $k \in N$, we clearly have the relationships

$$x^{k}(t_{i}^{k}) = x_{i}^{k} = t \to t_{i}^{k}$$
 and $\dot{x}_{i}^{k}(t) := V_{i+1}^{k}$ for all $t \in (t_{i}^{k}, t_{i+1}^{k})$. (15)

As discussed in [3], the solutions to (14) in the *uncontrolled* setting of (13) with g = g(x(t)) uniformly converge on $[0, \overline{T}_k]$ to a trajectory of a certain perturbed sweeping process. The *controlled* model under consideration here is significantly more involved. For all $x(t) \in \mathbb{R}^{2n}$, consider the set

$$:= \left\{ y(t) \in \mathbb{R}^{2n} \mid D_{ij}(x(t)) + \nabla D_{ij}(x(t)) \frac{(y(t) - x(t))}{(y(t) - x(t))} \right\} \quad \text{whenever } i < j \right\}, \tag{16}$$

which allows us to represent the algorithm in (13), (14) as

$$x_{i+1}^k = \Pi\left(x_i^k + h^k g(x_i^k, u_i^k); K(x_i^k)\right)$$
 for $i = 0, \dots, k-1$.

Thus it can be equivalently rewritten in the form of

$$x^{k}\left(\vartheta^{k}(t)\right) = \Pi\left(x^{k}(\tau^{k}(t)) + h^{k}g\left(x^{k}(\tau^{k}(t)), u^{k}(\tau^{k}(t))\right); K(x^{k}(\tau^{k}(t))\right)$$

for all $t \in [0, \overline{T}_k]$, where the functions $\tau^k(t) := t_i^k$ and $\vartheta^k(t) := t_{i+1}^k$ for all $t \in I_i^k$. Using the construction of the convex set K(x) in (16) and the definition of the normal cone together with the relationships in (15), we arrive at the sweeping process inclusions

$$\dot{x}^{k}(t) \in N\left(x^{k}(\vartheta^{k}(t)); K(x^{k}(\tau^{k}(t)))\right) + g\left(x^{k}(\tau^{k}(t)), u^{k}(\tau^{k}(t))\right) \quad \text{a.e. } t \in [0, \overline{T}]$$

$$\tag{17}$$

with $x^k(0) = x_0 \in K(x_0) = A$ and $x^k(\vartheta^k(t)) \in K(x^k(\tau^k(t)))$ on $[0,\overline{T}]$. To formalize (17) as a controlled perturbed sweeping process of type (2), we define the

convex polyhedron $C(t) \subset \mathbb{R}^{2n}$ by

$$C(t) := \bigcap \left\{ x(t) \in \mathbb{R}^{2n} \mid \langle x_*^j(t), x(t) \rangle \le c_j(t), j = 1, \dots, n - 1 \right\}$$
 (18)

with $c_j(t) := -(R_{obj} + R_{obs})$, where R_{obj} , R_{obs} are the radii of the designated object and the obstacle, respectively. The n-1 vertices of the polyhedron are given by

$$x_*^j := e_{j1} + e_{j2} - e_{(j+1)1} - e_{(j+1)2} \in \mathbb{R}^{2n}, \quad j = 1, \dots, n-1,$$
 (19)

where e_{ii} (j = 1, ..., n and i = 1, 2) are the vectors in \mathbb{R}^{2n} of the form

$$e := (e_{11}, e_{12}, e_{21}, e_{22}, \dots, e_{n1}, e_{n2}) \in \mathbb{R}^{2n}$$

with 1 at only one position of e_{ji} and 0 at all the other positions. In order to obtain the optimal solutions to the formulated problem by using Theorem 2.5 in what follows, we choose for convenience the norm $\|(x^{j1}, x^{j2})\| := |x^{j1}| + |x^{j2}|$ for each component $x^j \in \mathbb{R}^2$ of $x \in \mathbb{R}^{2n}$.

In the next two sections, we study in detail the two practical models, which have some common features described in the framework discussed above. The first model addresses optimal control of *marine surface vehicles* whose dynamics was described as a sweeping process in [7]. The second model concerns the *motion of nanoparticles*, where the dynamics is based on the sweeping process description taken from [3]. Note that both these models are essentially different from the corridor and planar versions of the microscopical *crowd motion model* described via the sweeping dynamics in [15], optimal control problems for such models were studied in [22, 39] based on necessary optimality conditions developed in [21, 39], respectively. In what follows, we present applications to the aforementioned new models based on the novel necessary optimality conditions derived in [36].

Let us emphasize here that the major differences between the new two models and the crowd motion model lie in the complexity of the dynamical systems involved. In particular, for the nanoparticle model, it is more than just the motions of two objects; this model is strongly influenced by other factors in the body. Indeed, the movement of nanoparticles is determined by the forces applied by the flow (bloodstream) and gravity. The forces influencing nanoparticles encompass hemodynamic forces, buoyancy, and Van der Waals interactions among nanoparticles, both inter-particle and with surrounding walls. Therefore, to have the velocities of the nanoparticles, we calculated all these factors, as detailed in Table 1 (on the last page). This integrated approach ensures a more precise and scientific understanding of nanoparticle dynamics in biological environments. The differences between the machine surface vehicle and nanoparticle models, as well as between their mathematical descriptions and optimality conditions for them are discussed below in Sections 4 and 5.

Table 1. Data of the nanoparticles inside a straight microtube.

634 635 636

637

638 639

640 641

642 643

644 645

Nanoparticle i	Data
i = 1	$dw_{1,1} = a - x^{12} - R_1 = 145$ $dw_{2,1} = a + x^{12} - R_1 = 845$
	$h_6^{m}(x^{12}) = 6\pi \mu R_1 \left[1 + \frac{9}{16} \left(\frac{n_1}{R_1 + dw_{1,1}} \right) + 0.13868 \left(\frac{n_1}{R_1 + dw_{1,1}} \right) \right] \approx 0.3267374$
	$h_6^{w_1}(x^{12}) = 6\pi \mu R_1 \left[1 + \frac{9}{16} \left(\frac{R_1}{R_1 + dw_{1,1}} \right) + 0.13868 \left(\frac{R_1}{R_1 + dw_{1,1}} \right)^{1.4829} \right] \approx 0.3267374$ $h_6^{w_2}(x^{12}) = 6\pi \mu R_1 \left[1 + \frac{9}{16} \left(\frac{R_1}{R_1 + dw_{2,1}} \right) + 0.13868 \left(\frac{R_1}{R_1 + dw_{2,1}} \right)^{1.4829} \right] \approx 0.3215246$
	$h_1^{w_1}(x^{12}) = \frac{48}{15}\pi \mu R_1 \left[ln \left(1 - \frac{R_1}{R_1 + dw_{1,1}} \right) + \frac{R_1}{R_1 + dw_{1,1}} \right] \approx -0.0000971$
	$h_1^{w_2}(x^{12}) = \frac{48}{15}\pi \mu R_1 \left[ln \left(1 - \frac{R_1}{R_1 + dw_{2,1}} \right) + \frac{R_1}{R_1 + dw_{2,1}} \right] \approx -0.0000030$
	$h_5^{W_1}(x^{12}) = h_5^{W_2}(x^{12}) = 6\pi \mu R_1 \left -\frac{1}{1 - \frac{R_1}{1 - \frac{1 - \frac{R_1}{1 - \frac{R_1}{1 - \frac{R_1}{1 - \frac{R_1}{1 - \frac{R_1}{1 - \frac{R_1}$
	$F_{1w} = \left \frac{AR_1^2}{dw_1^4} - \frac{AR_1^2}{dw_2^4} \right \approx 1.325e - 27$
	$F_{12} = \frac{AR_1^2}{\rho_1^4} \approx 4.139e - 28$, where $D_{12} = 197.1320344$
	$\int v^{11} = \frac{1}{dt} = \frac{1.036e + 13}{h_1^{w_1}(x^{12}) + h_1^{w_2}(x^{12})} \approx 1.036e + 13$
	$\begin{cases} v^{11} = \frac{1}{dt} \frac{dx^{11}}{dt} = \frac{-[h_6^{W_1}(x^{12}) + h_6^{W_2}(x^{12})]S}{h_1^{W_1}(x^{12}) + h_1^{W_2}(x^{12})} \approx 1.036e + 13\\ v^{12} = \frac{dx^{12}}{dt} = \frac{\frac{4\pi}{3}gR_1\Delta\rho + F_{12} + F_{1w}}{h_5^{W_1}(x^{12}) + h_5^{W_2}(x^{12})} \approx 3.154e + 14 \end{cases}$
	$\begin{cases} \text{ or } h_5^{-1}(x^{12}) + h_5^{-2}(x^{12}) \\ s_1 = 3.156e + 14 \end{cases}$
i = 2	$dw_{1,2} = a - x^{22} - R_2 = 290$
	$dw_{2,2} = a + x^{22} - R_2 = 690$
	$h_6^{w_1}(x^{22}) = 6\pi \mu R_2 \left[1 + \frac{9}{16} \left(\frac{R_2}{R_2 + dw_{1,2}} \right) + 0.13868 \left(\frac{R_2}{R_2 + dw_{1,2}} \right)^{1.4829} \right] \approx 0.6534748$
	$h_6^{w_2}(x^{22}) = 6\pi \mu R_2 \left[1 + \frac{9}{16} \left(\frac{R_2}{R_2 + dw_{2,2}} \right) + 0.13868 \left(\frac{R_2}{R_2 + dw_{2,2}} \right)^{1.4829} \right] \approx 0.6461981$
	$h_1^{w_1}(x^{22}) = \frac{48}{15}\pi \mu R_2 \left[ln \left(1 - \frac{R_2}{R_2 + dw_{12}} \right) + \frac{R_2}{R_2 + dw_{12}} \right] \approx -0.0001942$
	$h_1^{w_2}(x^{22}) = \frac{48}{15}\pi \mu R_2 \left[ln \left(1 - \frac{R_2}{R_2 + dw_{22}} \right) + \frac{R_2}{R_2 + dw_{22}} \right] \approx -0.0000352$
	$h_5^{W_1}(x^{22}) = h_5^{W_2}(x^{22}) = 6\pi \mu R_2 \left[\frac{1}{1 - \frac{R_2}{12}} + \frac{1}{8} ln \left(1 - \frac{R_2}{ x^{22} } \right) \right] \approx -0.6787248$
	$F_{2W} = \left \frac{AR_2^3}{dw_{1,2}^4} - \frac{AR_2^3}{dw_{2,2}^4} \right \approx 6.849e - 28$
	$F_{21} = \frac{AR_2^3}{\rho_2^4} \approx 3.311e - 27$, where $D_{21} = 197.1320344$
	$\begin{cases} v^{21} = \frac{dx^{21}}{dt} = \frac{-[h_6^{w_1}(x^{22}) + h_6^{w_2}(x^{22})]5}{h_1^{w_1}(x^{22}) + h_1^{w_2}(x^{22})} \approx 9.064e + 12 \\ v^{22} = \frac{dx^{22}}{dt} = \frac{\frac{dx^{22}}{3}gR_2\Delta\rho + F_{21} + F_{2w}}{h_5^{w_1}(x^{22}) + h_5^{w_2}(x^{22})} \approx 3.027e + 14 \end{cases}$
	$v^{22} = \frac{dx^{22}}{dx} = \frac{\frac{4\pi}{3}gR_2\Delta\rho + F_{21} + F_{2w}}{\frac{W_{12}}{3}gR_2\Delta\rho + \frac{W_{22}}{3}gR_2\Delta\rho} \approx 3.027e + 14$
	$ \int_{5_2} dt h_5^{m_1}(x^{22}) + h_5^{m_2}(x^{22}) $ $ s_2 = 3.0284e + 14 $

Note furthermore that in these two new optimal control models, the necessary optimality conditions from [36] not only allow us to get the shortest path but also provide minimizing the duration of the dynamic process, which has not been considered before in the settings of the crowd motion and other models involving the sweeping dynamics. This difference has significant practical implications for the applications. In the context of marine vehicles, if optimization of travel time is not addressed, each vehicle may proceed leisurely to its destination, although along the optimal trajectory. Such an approach not only leads us to the excessive fuel consumption but also fails to deliver economic efficiency, resulting in additional negative consequences. Efficiently optimizing the time of movements

647

648 649 650

651 652

653

654

655

656

657

658

659

660

661

662

663

664

665 666

667

668

669 670

671 672

673

674

675

676

677

678

679

680

681

682 683

684 685 686

687 688 is crucial for maximizing performance and minimizing costs enhancing thereby the overall effectiveness of maritime operations as well as boosting advancements in pharmaceutical and therapeutic practices.

4. Optimal control of marine surface vehicles

In this section, we explore the dynamic movements of unmanned surface vehicles (USVs) with diverse shapes as they navigate through maritime environments. These USVs are not only capable of reaching their destinations safely but also adept at avoiding both stationary and moving obstacles. This modelling approach transforms the scenario into a controlled perturbed sweeping process using the procedure established in Section 3, which treats each USV as an object within the dynamic system alongside n-1 other obstacles on the way to reach the target. This framework finds practical applications in a variety of real-world scenarios, such as oceanographic research, environmental monitoring, maritime surveillance, and autonomous shipping while showcasing the versatility and adaptability of unmanned surface vehicles across different domains.

Note that, in the absence of obstacles, the desired velocities are given by $V(x) = g(x) \in \mathbb{R}^{2n}$. In the presence of obstacles, we take into account the algorithmic developments of [7] and seek optimal velocities to escape from different surrounding obstacles by solving the following convex constrained optimization problem:

minimize
$$||g(x, u) - V(x)||^2$$

subject to $V(x) \in C_h(x)$, (20)

where the control *u* is involved into the desired velocity term to adjust the actual velocities of the USVs and make sure that they do not overlap. The algorithmic design in (20) means that V_{k+1} is selected as the (unique) element from the set of admissible velocities as the closest one to the desired velocity g(x, u) in order to avoid the overlapping. Consequently, the proposed scheme seeks new directions V(x) of USVs close to the desired direction g(x, u) in order to by pass the surrounding obstacles. The desired position of the next configuration of marine vessels is then generated as $x_{\text{ref}}(t+h) = (x_{\text{ref}}, y_{\text{ref}}) = x(t) + hV(x)$, and the desired via point posture position of the designated marine craft is given by

$$\eta_{\text{ref}} = (x_{\text{ref}}, y_{\text{ref}}, \psi_{\text{ref}}), \text{ where } \psi_{\text{ref}} := \tan^{-1} \left(\frac{y_{\text{ref}i} - y_i(t)}{x_{\text{ref}i} - x_i(t)} \right).$$

With the constructions in Section 3, we now formulate the sweeping optimal control problem (P) that can be treated as a continuous-time counterpart of the discrete algorithm of the marine surface vehicles model by taking into account the model goals discussed above. Consider the cost functional

minimize
$$J[x, u, T] := \frac{1}{2} ||x(T)||^2 + \frac{1}{2} T^2,$$
 (21)

 which reflects the model goals to minimize the distance and the time for the USV to achieve the target from the admissible configuration set. We describe the continuous-time dynamics by the controlled sweeping process

$$\begin{cases} -\dot{x}(t) \in N(x(t); C(t)) + g(x(t), u(t)), \\ x(0) = x_0 \in C(0), \ u(t) \in U, \end{cases}$$
 (22)

for a.e. $t \in [0, T]$, where the constant set C(t) is taken from (18), the control constraints reduce to (12), and the dynamic nonoverlapping condition $||x^{i}(t)||$ $|x^{j}(t)|| \geq R_i + R_j$ is equivalent to the pointwise state constraints

$$x(t) \in C(t) \iff \langle x_*^j(t), x(t) \rangle \leq c_j(t) \quad \text{for all } t \in [0, T] \quad \text{and } j = 1, \dots, n-1,$$

which follow from the construction of C(t) and the normal cone definition.

From now on, we exclusively study the sweeping optimal control problem defined in (21) and (22) with the marine surface vehicles model data specified below. Applying Theorem 2.5 allows us to obtain the necessary optimality conditions for the problem that are formulated entirely in terms of the model data.

Consider the two marine crafts (MCs), MC 1 and MC 2, as moving vehicles. The marine surface vehicles are represented by triangle shapes immersed in discs Figure 1. The objective is to move MC 1 and MC 2 to the target without colliding with each other. However, in the presence of MC 2, after the contacting time t^* the vehicle MC 1 pushes MC 2 to the target together with the same velocity. The mathematical USV model is taken from the physical ship called Cyber-Ship [46] with the mass of 23.8 kg and the length of 1.255 m. The initial configuration is $x(0) = (x^1(0), x^2(0))$, where $x^1(0)$ is the initial position of MC 1 and $x^2(0)$ is the initial position of MC 2. The position of the target is the origin. The radii of different discs used in this model are chosen as $R_1 = R_2 = 3.5$ m. We specify the other model data as follows:

$$\begin{cases} n = 2, x(0) = (x^{1}(0), x^{2}(0)), x_{*}(t) = (1, 1, -1, -1), c(t) = -7 \text{ for all } t, \\ g(x, u) := u, \varphi(x, T) := \frac{1}{2} ||x(T)||^{2} + \frac{1}{2} T^{2}, s_{1} = s_{2} = 1, \\ U = \left\{ u(t) = (u^{1}(t), u^{2}(t)) \in \mathbb{R}^{4} \mid ||u^{1}(t)|| \le 100, ||u^{2}(t)|| \le 60 \right\}, \\ \theta^{u} := \theta_{1}^{u} = \theta_{2}^{u} = 45^{\circ}, x^{1}(0) = (-25, -25), x^{2}(0) = (-15, -15). \end{cases}$$
(23)

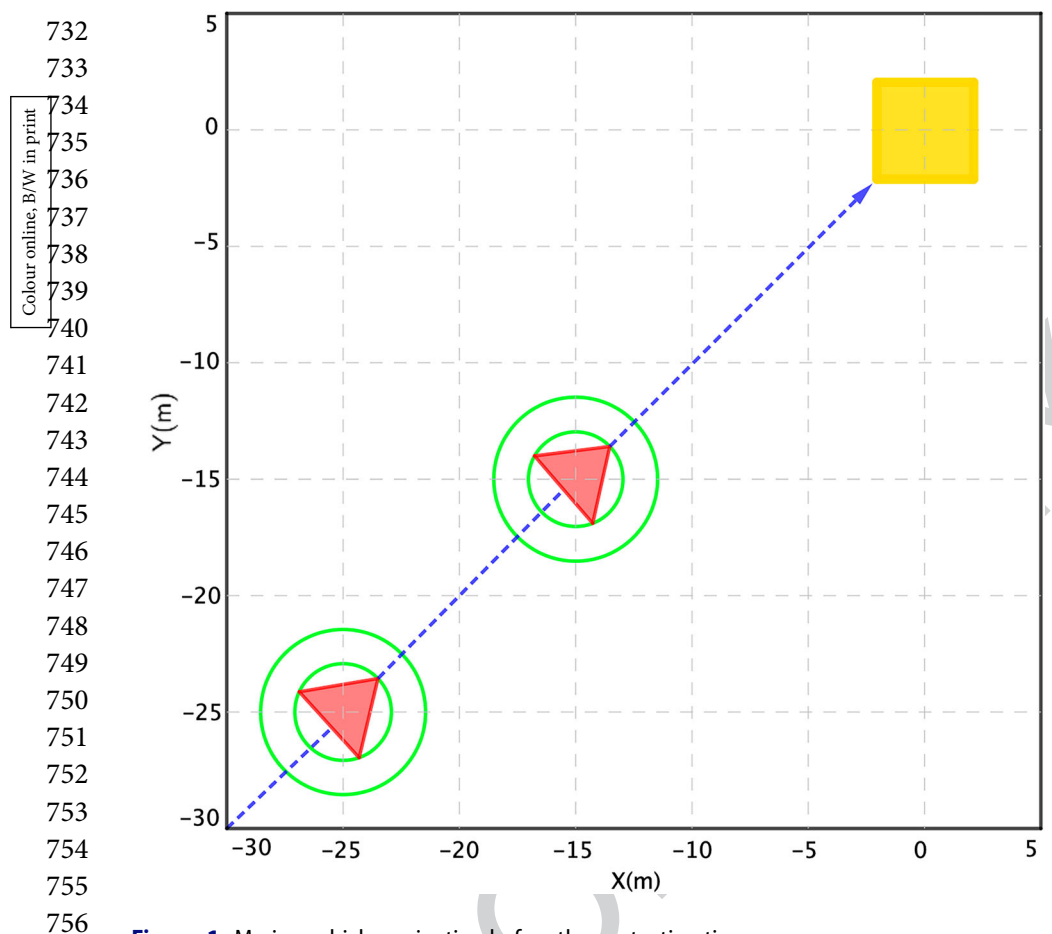


Figure 1. Marine vehicle navigation before the contacting time.

The moving set C(t) in the sweeping inclusion (22) is described now by

$$C(t) = \left\{ x \in \mathbb{R}^4 \mid \langle x_*(t), x \rangle \le c(t) \right\}$$

$$= \left\{ x \in \mathbb{R}^4 \mid x^{11} + x^{12} - x^{21} - x^{22} \le -7 \right\}$$

$$= \left\{ x \in \mathbb{R}^4 \mid |x^{21} - x^{11}| + |x^{22} - x^{12}| \ge 7 \right\}$$
(under the imposed assumptions $x^{21} > x^{11}$ and $x^{22} > x^{12}$)
$$= \left\{ x \in \mathbb{R}^4 \mid ||x^2 - x^1|| \ge 2R \right\} \quad \text{for all } t \in [0, T].$$

The structure of the problem in (22) and (23) suggests that the object changes its velocity only when it hits the boundary at some time t_m with $m \in \{0, 1, ..., k\}$. If furthermore $t_m < T$, the object slides on the boundary of C(t) for the entire time interval $[t_m, T]$.

Observing that the controlled sweeping process in (22), (23) satisfies all the assumptions of Theorem 2.5, we have the following relationships to find optimal solutions $\bar{x}(t) = (\bar{x}^1(t), \bar{x}^2(t)), \bar{u}(t) = (\bar{u}^1(t), \bar{u}^2(t)), \text{ and } \overline{T}.$



775
776
(1)
$$\dot{\bar{x}}(t) = \begin{cases} \bar{u}(t) - \eta_0(1, 1, -1, -1) & \text{if } t \in (0, t_m), \\ \bar{u}(t) - \eta_m(1, 1, -1, -1) & \text{if } t \in (t_m, \overline{T}) \\ \text{with } \eta_0, \eta_m \ge 0. \end{cases}$$
778
(2) $\dot{p}(t) = 0$ for a $t \in [0, \overline{T}]$

(2) $\dot{p}(t) = 0$ for a.e. $t \in [0, \overline{T}]$.

- (3) $q(t) = p(t) \epsilon t_t^{\overline{T}} d\gamma(\tau)(1, 1, -1, -1).$
- (4) $\psi(t) = q(t) \in N(\bar{u}(t); U) \text{ a.e. } t \in [0, \overline{T}].$
 - (5) $\langle \psi(t), \bar{u}(t) \rangle = \max_{u \in U} \langle \psi(t), u \rangle$ a.e. $t \in [0, \overline{T}]$, which can be rewritten as

$$\langle \psi_1(t), \bar{u}^1(t) \rangle + \langle \psi_2(t), \bar{u}^2(t) \rangle = \max_{(u^1, u^2) \in U} \left\{ \langle \psi_1(t), u^1 \rangle + \langle \psi_2(t), u^2 \rangle \right\},\,$$

where $\psi_1(t) = (\psi_{11}(t), \psi_{12}(t))$ and $\psi_2(t) = (\psi_{21}(t), \psi_{22}(t))$.

(6)
$$\eta(t) \ge 0$$
, $\|\bar{x}^2 - \bar{x}^1\| > 7 \Longrightarrow \eta(t) = 0$ for a.e. $t \in [0, \overline{T}]$.

(7)
$$\eta(t) > 0 \Longrightarrow \|\bar{x}^2 - \bar{x}^1\| = 7 \text{ a.e. } t \in [0, \overline{T}].$$

(8)
$$\begin{cases}
-p(\overline{T}) = \eta(\overline{T})(1, 1, -1, -1) + \mu \bar{x}(\overline{T}), \, \eta(\overline{T}) \ge 0, \\
\eta(\overline{T}) > 0 \Longrightarrow \|\bar{x}^1(\overline{T}) + \bar{x}^2(\overline{T})\| = 7, \\
\frac{1}{T} \in t_0^{\overline{T}} \langle p(t), \dot{x}(t) \rangle \, \mathrm{d}t = \mu \overline{T}.
\end{cases}$$

(9)
$$\begin{cases} (\mu, p, \|\gamma_0\|_{TV}, \|\gamma_0\|_{TV}) \neq 0, & \mu \geq 0, \\ \mu = 1 \text{ if } \langle (1, 1, -1, -1), \bar{x}(t) \rangle < -7 \text{ on } [0, \overline{T}]. \end{cases}$$

(9)
$$\begin{cases} (\mu, p, \|\gamma_0\|_{TV}, \|\gamma_>\|_{TV}) \neq 0, & \mu \geq 0, \\ \mu = 1 \text{ if } \langle (1, 1, -1, -1), \bar{x}(t) \rangle < -7 \text{ on } [0, \overline{T}]. \\ \sup_{t \in T} (10) & \sup_{t \in T} (\gamma_>) \cap \inf_{t \in T} (E_0) = \emptyset \text{ if } \inf_{t \in T} (E_0) = \inf_{t \in T} (\{t \mid \eta(t) > 0\}) \neq \emptyset. \end{cases}$$

By condition 2, p(t) is constant on $[0, \overline{T}]$. Substituting it into 3 yields

$$q(t) = p(\overline{T}) - \in t_t^{\overline{T}}(1, 1, -1, -1) \, d\gamma(\tau) = p(\overline{T}) - (1, 1, -1, -1)\gamma([t, \overline{T}]). \tag{24}$$

Then combining (24) and 8 gives us the expression

$$q(t) = -\mu \bar{x}(\overline{T}) - (1, 1, -1, -1) \left(\eta(\overline{T}) + \gamma \left([t, \overline{T}] \right) \right) \quad \text{on } [0, \overline{T}].$$

Since we start from an interior point of the polyhedron, the measure γ is zero in the interval $[0, t_m]$. Let us investigate behaviour of the trajectory before and after the hitting time $t = t_m$. Remembering that the trajectory does not hit the boundary before $t = t_m$, it follows from 6 that $\gamma([t, T]) \equiv \gamma([t_m, \overline{T}])$ for all $t \in$ $[0,t_m)$. Thus

$$q(t) \equiv -\mu \bar{x}(\overline{T}) - (1, 1, -1, -1) \left(\eta(\overline{T}) + \gamma \left([t_m, \overline{T}] \right) \right) =: r_m = (r_{1m}, r_{2m}) \in \mathbb{R}^4$$
(25)

for all $t \in [0, t_m)$. From now on, we suppose for determinacy and simplicity in this complicated model that optimal control under consideration is constant on $[0, \overline{T}]$ and belong to the interior of *U*. Combining 4 and 5 tells us that

$$\langle r_{1m}, \bar{u}^1 \rangle + \langle r_{2m}, \bar{u}^2 \rangle = \max_{(u^1, u^2) \in U} \left\{ \langle r_{1m}, u^1 \rangle + \langle r_{2m}, u^2 \rangle \right\},$$

which can be written by (25) in the form

819
820
$$\langle -\mu \bar{x}^{1}(\overline{T}) - (1,1)(\eta(\overline{T}) + \gamma([t_{m}, \overline{T}])), \bar{u}^{1} \rangle$$
821
$$+ \langle -\mu \bar{x}^{2}(\overline{T}) - (-1,-1)(\eta(\overline{T}) + \gamma([t_{m}, \overline{T}])), \bar{u}^{2} \rangle$$
822
$$= \max_{(u^{1},u^{2})\in U} \{ \langle -\mu \bar{x}^{1}(\overline{T}) - (1,1)(\eta(\overline{T}) + \gamma([t_{m}, \overline{T}])), u^{1} \rangle$$
824
$$+ \langle -\mu \bar{x}^{2}(\overline{T}) - (-1,-1)(\eta(\overline{T}) + \gamma([t_{m}, \overline{T}])), u^{2} \rangle \}$$

According to the above, consider the linear function

$$\phi(u^{1}, u^{2}) := \left\langle -\mu \bar{x}^{1}(\overline{T}) - (1, 1)(\eta(\overline{T}) + \gamma([t_{m}, \overline{T})), u^{1} \right\rangle + \left\langle -\mu \bar{x}^{2}(\overline{T}) - (-1, -1)(\eta(\overline{T}) + \gamma([t_{m}, \overline{T}])), u^{2} \right\rangle,$$

which attains its maximum over U at the interior point (\bar{u}_1, \bar{u}_2) . Thus the Fermat rule for ϕ gives us the conditions

$$-\mu \bar{x}^1(\overline{T}) = (1,1)(\eta(\overline{T}) + \gamma([t_m, \overline{T}])) \text{ and}$$

$$\mu \bar{x}^2(\overline{T}) = (1,1)(\eta(\overline{T}) + \gamma([t_m, \overline{T}])),$$

which imply in turn the equalities

$$-\bar{x}^1(\overline{T}) = \bar{x}^2(\overline{T}) = (1,1)(\eta(\overline{T}) + \gamma([t_m, \overline{T}])). \tag{26}$$

When the particle moving hits the boundary at the time $t = t_m$, it follows from **6** that

$$|\bar{x}^{21}(t_m) - \bar{x}^{11}(t_m)| + |\bar{x}^{22}(t_m) - \bar{x}^{12}(t_m)| = 7, \text{ and}$$

$$\eta(t) = \begin{cases} \eta_0 = 0 & \text{if } t \in [0, t_m], \\ \eta_m \ge 0 & \text{if } t \in [t_m, \overline{T}]. \end{cases}$$

After the hitting point, both these marine USVs will move to the target under the control \bar{u} . This yields

$$\begin{cases} \bar{x}^{1}(t) = \left(-25 + t\|\bar{u}^{1}\|\cos\theta^{u}, -25 + t\|\bar{u}^{1}\|\sin\theta^{u}\right), \\ \bar{x}^{2}(t) = \left(-15 + t\|\bar{u}^{2}\|\cos\theta^{u}, -15 + t\|\bar{u}^{2}\|\sin\theta^{u}\right) \end{cases}$$

for $t \in [0, t_m)$ as well as the representations

856
857
858
859
860
$$\begin{cases}
\bar{x}^{1}(t) = \left(-25 + t_{m} \|\bar{u}^{1}\| \cos \theta^{u} + (t - t_{m})(\|\bar{u}^{1}\| \cos \theta^{u} - \eta_{m}), \\
-25 + t_{m} \|\bar{u}^{1}\| \sin \theta^{u} + (t - t_{m})(\|\bar{u}^{1}\| \sin \theta^{u} - \eta_{m})\right), \\
\bar{x}^{2}(t) = \left(-15 + t_{m} \|\bar{u}^{2}\| \cos \theta^{u} + (t - t_{m})(\|\bar{u}^{2}\| \cos \theta^{u} + \eta_{m}), \\
-15 + t_{m} \|\bar{u}^{2}\| \sin \theta^{u} + (t - t_{m})(\|\bar{u}^{2}\| \sin \theta^{u} + \eta_{m})\right)
\end{cases}$$

for $t \in [t_m, \overline{T}]$. Recalling that the normal vectors are inactive before the hitting time, we arrive at the equality

$$2\left|10 + \frac{\sqrt{2}}{2}t_m(\|\bar{u}^2\| - \|\bar{u}^1\|) + (t - t_m)\left(\frac{\sqrt{2}}{2}(\|\bar{u}^2\| - \|\bar{u}^1\|) + 2\eta_m\right)\right|$$

$$= 7 \quad \text{if } t \ge t_m$$

for the time of contact. This brings us to the equation

$$\left|10 - \frac{\sqrt{2}}{2}t_m(\|\bar{u}^2\| - \|\bar{u}^1\|)\right| = 7,$$

which has the following two solutions:

$$t_m = \frac{-13}{\sqrt{2}(\|\bar{u}^2\| - \|\bar{u}^1\|)}$$
 and $t_m = \frac{-27}{\sqrt{2}(\|\bar{u}^2\| - \|\bar{u}^1\|)}$ (27)

with $\|\bar{u}^2\|<\|\bar{u}^1\|$, which will both be checked for the optimality below. When $\bar{x}(\cdot)$ hits the boundary of C, it would stay there while pointing in the direction shown in Figure 2. Thus we get

$$\frac{\sqrt{2}}{2}(\|\bar{u}^2\| - \|\bar{u}^1\|) + 2\eta_m = 0, \quad \text{and so } \eta_m = \frac{\sqrt{2}(\|\bar{u}^1\| - \|\bar{u}^2\|)}{4}. \tag{28}$$

Furthermore, it follows from (26) that the optimal time is calculated by

$$\overline{T} = \frac{40\sqrt{2}}{\|\bar{u}^2\| + \|\bar{u}^1\|}.$$

Since $p(\cdot)$ is constant on $[0, \overline{T}]$, the third condition in 8 yields

$$\frac{1}{\overline{T}} \in t_0^{\overline{T}} \langle p(\overline{T}), \dot{\overline{x}}(t) \rangle \, \mathrm{d}t = \mu \, \overline{T}, \quad \text{i.e. } p(\overline{T}) \, \overline{x}(\overline{T}) = \mu \, \overline{T}^2. \tag{29}$$

To get enough information, suppose that $\mu = 1$. Substituting (29) into the first equation in 8 yields

$$-\eta_m(1, 1, -1, -1) = \bar{x}(\overline{T}) + \frac{\overline{T}^2}{\bar{x}(\overline{T})}.$$
 (30)

With (27) and η_m taken from (27) and (28), respectively, the cost function value at (30) is

$$\int [\bar{x}, \bar{u}, \overline{T}] = -25 + \frac{\sqrt{2}}{2} t_m \|\bar{u}^1\| + (t - t_m) \left(\frac{\sqrt{2}}{2} \|\bar{u}^1\| - \eta_m \right)^2 + -15 + \frac{\sqrt{2}}{2} t_m \|\bar{u}^2\| + (t - t_m) \left(\frac{\sqrt{2}}{2} \|\bar{u}^2\| + \eta_m \right)^2 + \frac{1}{2} \overline{T}^2.$$

When the object hits the boundary, it then slights there until the end of the process, i.e. $t \ge t_m$. It then follows that $\eta_m > 0$. By using computer calculations, all

905 906

923

924

925

926 927

928

929 930 931

932

937 938

939 940

941 942

943

944

945 946 the cases can be analysed. This shows that the best performance is obtained by choosing the contacting time $t_m = \frac{-13}{\sqrt{2}(\|\bar{u}^2\| - \|\bar{u}^1\|)}$ for which we have

$$J[\bar{x}, \bar{u}, \bar{T}]$$
908
909
$$= \left[-25 + \frac{-13\|\bar{u}^1\|}{2(\|\bar{u}^2\| - \|\bar{u}^1\|)} + \left(\frac{40\sqrt{2}}{\|\bar{u}^2\| + \|\bar{u}^1\|} - \frac{-13}{\sqrt{2}(\|\bar{u}^2\| - \|\bar{u}^1\|)} \right) \right]$$
911
$$\left(\frac{\sqrt{2}}{2} \|\bar{u}^1\| - \frac{\sqrt{2}(\|\bar{u}^1\| - \|\bar{u}^2\|)}{4} \right) \right]^2$$
913
$$+ \left[-15 + \frac{-13\|\bar{u}^2\|}{2(\|\bar{u}^2\| - \|\bar{u}^1\|)} + \left(\frac{40\sqrt{2}}{\|\bar{u}^2\| + \|\bar{u}^1\|} - \frac{-13}{\sqrt{2}(\|\bar{u}^2\| - \|\bar{u}^1\|)} \right) \right]$$
917
918
$$\left(\frac{\sqrt{2}}{2} \|\bar{u}^2\| + \frac{\sqrt{2}(\|\bar{u}^1\| - \|\bar{u}^2\|)}{4} \right) \right]^2$$
920
921
$$+ \frac{1}{2} \left(\frac{40\sqrt{2}}{\|\bar{u}^2\| + \|\bar{u}^1\|} \right)^2.$$

This function achieves the minimum value $I \approx 6.1875$ at $\|\bar{u}^1\| \approx 99.9999$, $\|\bar{u}^2\| \approx 59.9999$, and $\overline{T} \approx 0.35355$, which imply that $t_m \approx 0.2298$ and $\bar{x}(\overline{T}) \approx 0.35355$ (-1.7502, -1.7502, 1.7498, 1.7498). This tells us that under the imposed assumptions we arrive at the unique optimal control $(\bar{u}^1, \bar{u}^2) \approx (70.7106, 70.7106,$ 42.4263, 42.4263). The corresponding optimal trajectory is

$$\begin{cases} \bar{x}^1(t) \approx (-25 + 70.7106t, -25 + 70.7106t), \\ \bar{x}^2(t) \approx (-15 + 42.4263t, -15 + 42.4263t) \end{cases}$$

for $t \in [0, 0.2298)$, and finally

$$\begin{cases} \bar{x}^1(t) \approx (-21.7500 + 56.5685t, -21.7500 + 56.5685t), \\ \bar{x}^2(t) \approx (-18.2500 + 56.5685t, -18.2500 + 56.5685t) \end{cases}$$

for the last interval $t \in [0.2298, 0.35355]$.

5. Applications to nanoparticles

The motivation to explore the motion of nanoparticles in a straight tube is driven by the profound influence of nanotechnology and biotechnology on pharmacology. This impact has significantly enhanced the performance of existing drugs while also enabling the development and utilization of novel drugs and therapies. Recognizing the transformative effects of these technologies on drug delivery and treatment strategies, this section seeks to understand and optimize the motion of nanoparticles within a confined space. Our research is motivated



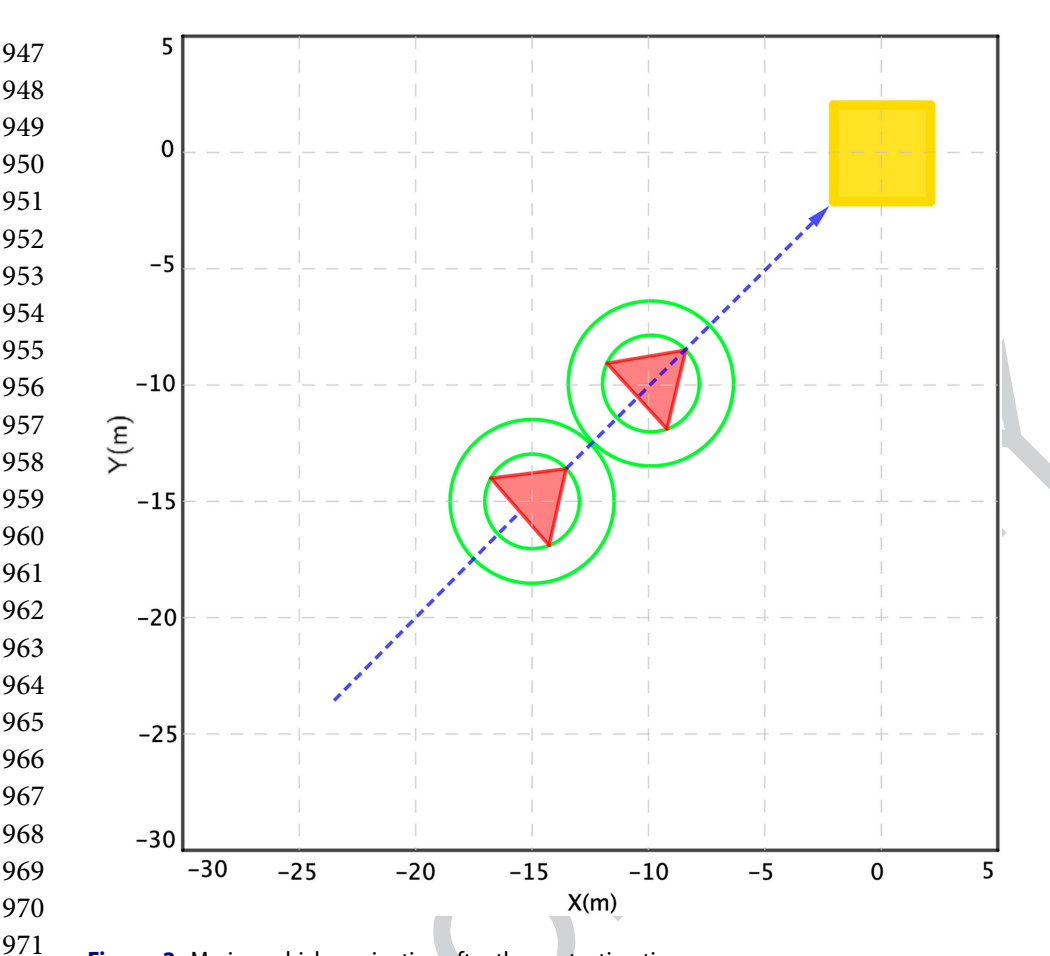


Figure 2. Marine vehicle navigation after the contacting time.

974 975

976

977

978

979

980

981

982

983

984

985

986

987

988 989 by the potential applications of such motion in improving drug delivery precision, facilitating controlled release mechanisms, and ultimately contributing to advancements in pharmaceutical and therapeutic practices. We study a scenario involving nanoparticles characterized as inelastic disks with varying radii. The objective for each nanoparticle is to traverse straight circular capillaries and reach the target at the end of the tube, in the shortest time. Throughout this motion, the nanoparticles potentially make contact with the other n-1 nanoparticles and treat them as obstacles while avoiding collisions.

For simplicity, taking into account the assumptions in [3] that the motion of the nanoparticles is considered on the xz-plane, i.e. the nanoparticle inelastic disk centre is always in the y = 0 plane, and there is no rotation of the nanoparticle about the z-axis. The nanoparticle therefore has two degrees of freedom: its motion is fully described by specifying (x^{i1}, x^{i2}) as functions of time t, where x^{i1} and x^{i2} are coordinates of the centre of nanoparticle i. The trajectory of each nanoparticle is governed by the forces exerted by the flow (blood stream) and the gravitation. Forces acting on nanoparticles include hemodynamic forces,

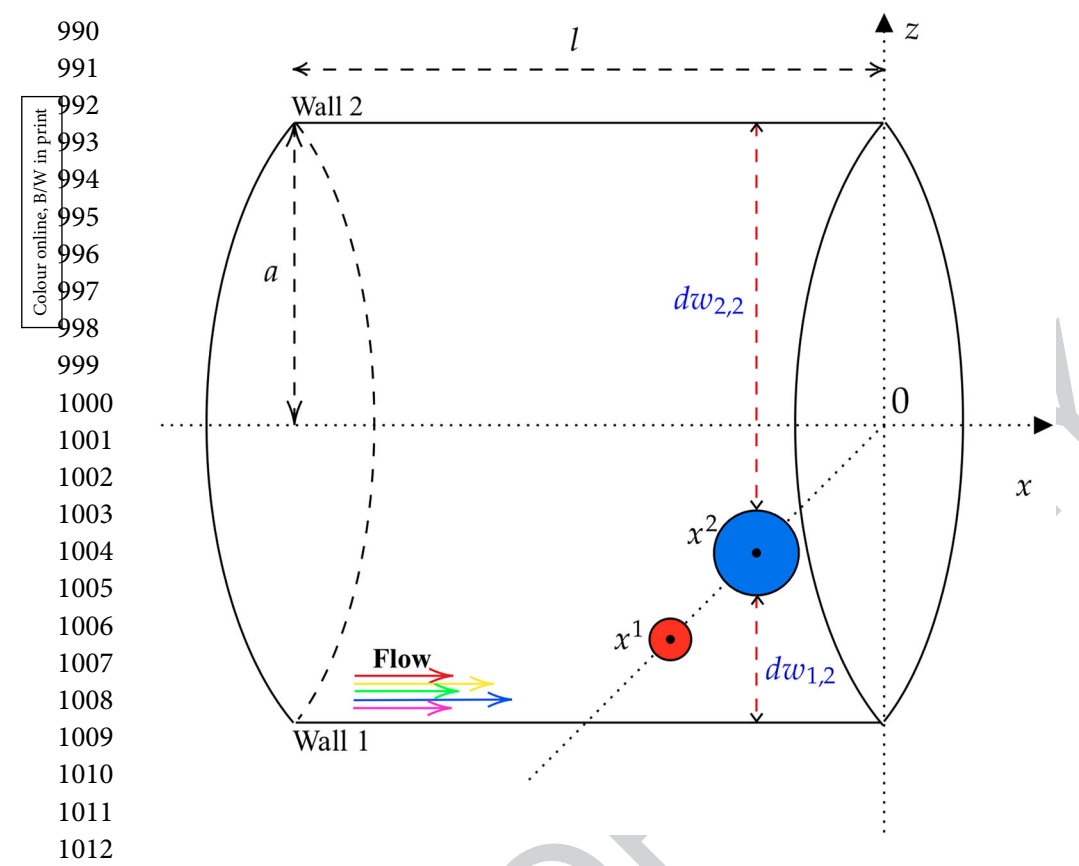


Figure 3. Nanoparticles in a straight tube.

buoyancy, Van der Waals' interactions between nanoparticles each-to-other and between nanoparticles and walls. To derive the equations describing the motion on the x-axis and on the z-axis, we apply (as suggested in [47]) the balance principle of forces acting on the nanoparticles. As considered in [48], the balance of forces acting on the nanoparticles requires, for each nanoparticle i, a system of two equations on the x-axis and the z-axis; see Figure 3.

Since all the nanoparticles intend to reach the end of the straight circular capillaries by the shortest path, their desired spontaneous (i.e. in the absence of other obstacles) velocities can be represented as

$$S(x) = (s_1, ..., s_n), \text{ with } s_i = (s_{x^{i1}}, s_{x^{i2}}), \text{ for } i = 1, ..., n,$$

where the velocity of nanoparticles are obtained after solving the following ODE system from [3]:

$$\begin{cases} \frac{\mathrm{d}x^{i1}}{\mathrm{d}t} = \frac{-\left[h_6^{w_1}(x^{i2}) + h_6^{w_2}(x^{i2})\right]S}{h_1^{w_1}(x^{i2}) + h_1^{w_2}(x^{i2})} \\ \frac{\mathrm{d}x^{i2}}{\mathrm{d}t} = \frac{\frac{4\pi}{3}gR\Delta\rho + \sum_{j\neq i}F_{ij} + F_{iw}}{h_5^{w_1}(x^{i2}) + h_5^{w_2}(x^{i2})} \end{cases}$$
for $i = 1, \dots, n$.

Here S is the shear rate of the flow, $h_1^{w_k}$ and $h_6^{w_k}$ are the hemodynamic resistant force induced by the wall w_k on the x-axis, $h_5^{w_k}$ is the hemodynamic resistant force induced by the wall w_k on the z-axis (k = 1, 2), F_{ii} is the force exerted over nanoparticle *i* due to van der Waals' interaction energy between the nanoparticle i and nanoparticle j, and F_{iw} is the force exerted over nanoparticle i due to van der Waals' interaction energy between the nanoparticle *i* and the walls, i.e.

$$F_{iw} = |F_{iw_1} - F_{iw_2}|,$$

where F_{iw_k} is the force exerted over nanoparticle i due to van der Waals' interaction energy between the nanoparticle i and the wall k. It is known that

$$F_{ij} = \frac{AR_i^3}{D_{ij}^4},$$

where D_{ij} is the distance between the nanoparticles i and j. In the equations above, R_i denotes the radius of nanoparticle i, Δ_ρ stands for the difference between mass densities of the nanoparticles and the fluid, and g is the standard gravitational acceleration.

Now we introduce the sweeping optimal control problem (*P*) for the nanoparticles model discussed above. This formulation considers the aforementioned model objective and utilizes the modelling framework developed in Section 3. Similarly to Section 4, define the cost functional

minimize
$$J[x, u, T] := \frac{1}{2} ||x(T)||^2 + \frac{1}{2} T^2,$$
 (31)

which reflects the model goals to minimize the distance of the nanoparticle from the admissible configuration set to the end of the straight circular capillaries together with minimizing the time to reach the target. Employing the nonoverlapping algorithm introduced in [10] for the study of inelastic collision (see also [15, 20] for further developments in other models) and taking into account the above discussions, we describe the continuous-time dynamics by the controlled sweeping process

$$\begin{cases} \dot{x}(t) \in -N(x(t); C(t)) + g(x(t), u(t)) \text{ a.e. } t \in [0, T], \\ x(0) = x_0 \in C(0) \subset \mathbb{R}^{2n}, \\ u(t) \in U \text{ a.e. } t \in [0, T], \end{cases}$$
(32)

where the control constraints reduce to (12), and the dynamic nonoverlapping condition $||x^{i}(t) - x^{j}(t)|| \ge R_i + R_j$ is used to formulate the moving set

$$C(t) := \left\{ x(t) \in \mathbb{R}^{2n} \mid \langle x_*^j(t), x(t) \rangle \le c_j(t), j = 1, \dots, n - 1 \right\}$$
 (33)

with $c_i(t) := -(R_{nano} + R_{obs})$, where R_{nano} , R_{obs} are the radii of the considered nanoparticle and the obstacle, respectively. The n-1 vertices of the polyhedron are constructed as in (19).

1077

1078 1079

1080

1081

1082 1083

1084

1085

1091

1098

1099

1100

1101

1102 1103

1104

1105 1106 1107

1108

1109 1110

1111

1112 1113 1114

1115

1116

1117

1118

Observe that, although the frameworks of nanoparticle and marine USV models are rather similar, these two models are essentially different. The difference between them lie in both dynamics and constraints. In particular, the motion of nanoparticles is governed by the forces exerted by the flow (such as the bloodstream) and gravity. The forces influencing nanoparticles encompass hemodynamic forces, buoyancy, as well as Van der Waals' interactions, occurring among nanoparticles, both inter-particle and with surrounding walls. Consequently, to have the velocities of the nanoparticles, we should take into account all these factors, which are presented in Table 1.

Our initial data for the nanoparticle model are given as follows:

```
1086
1087
              n = 2, l = 7\mu m = 7000nm, h = 0.0075, R_1 = 5nm,
1088
              R_2 = 10nm, S = 1600e6 s^{-1},
1089
              A = 5e - 21, g = 9.81e9, \mu = 3.4e - 3, \Delta \rho = -1e3,
1090
              a = 0.5 \mu m = 500 nm,
              x_* = (1, 1, -1, -1), x(0) = (x^{11}(0), x^{12}(0), x^{21}(0), x^{22}(0)),
1092
              c = -R_1 - R_2 = -15,
1093
1094
              g(x, u) := u, \varphi(x, T) := \frac{1}{2} ||x(T)||^2 + \frac{1}{2} T^2,
1095
             U := \left\{ u = (u^1, u^2) \in \mathbb{R}^4 | \|u^1\| \in [0, 3], \|u^2\| \in [0, 3] | \|u^1\| = 2\|u^2\| \right\},

\theta^u = 45^\circ, x^1(0) = (-350, -350), x^2(0) = (-200, -200).
1096
1097
                                                                                                                 (34)
```

The data for nanoparticles in the viscous flow inside a tube with length *l*, width a, and parameters h, R_1 , R_2 , T, A, g, μ , and Δ_p are taken from [3]. The data for Sand related parameters reflected in Figure 4 are taken from [49]. The controlled desired velocities are naturally described by

$$g(x(t), u(t)) = u(t) = (s_1 || u^1(t) || \cos \theta^u(t),$$

$$s_1 || u^1(t) || \sin \theta^u(t), s_2 || u^2(t) || \cos \theta^u(t), s_2 || u^2(t) || \sin \theta^u(t)).$$

Table 1 collects the results of calculations of the model ingredients according to the above formulas with the data of (34) for two nanoparticles i = 1, 2.

At the initial time, we have $(x^{11}(0) - x^{21}(0))^2 + (x^{12}(0) - x^{22}(0))^2 = 45,000$. Let $t_* > 0$ stand for the first contacting time between the two nanoparticles, i.e.

$$t_* := \min \{ t \in [0, T] \mid ||\bar{x}^1(t) - \bar{x}^2(t)|| = R_1 + R_2 \}.$$

Recall that the nanoparticle tends to keep its constant direction and velocity until either touching the other nanoparticle (obstacle), or reaching the end of the straight microtube at $t = \overline{T}$. To proceed further, suppose that $\mu > 0$ for definiteness and apply the necessary optimality conditions of Theorem 2.5 in our control model. We arrive at the following relationships:

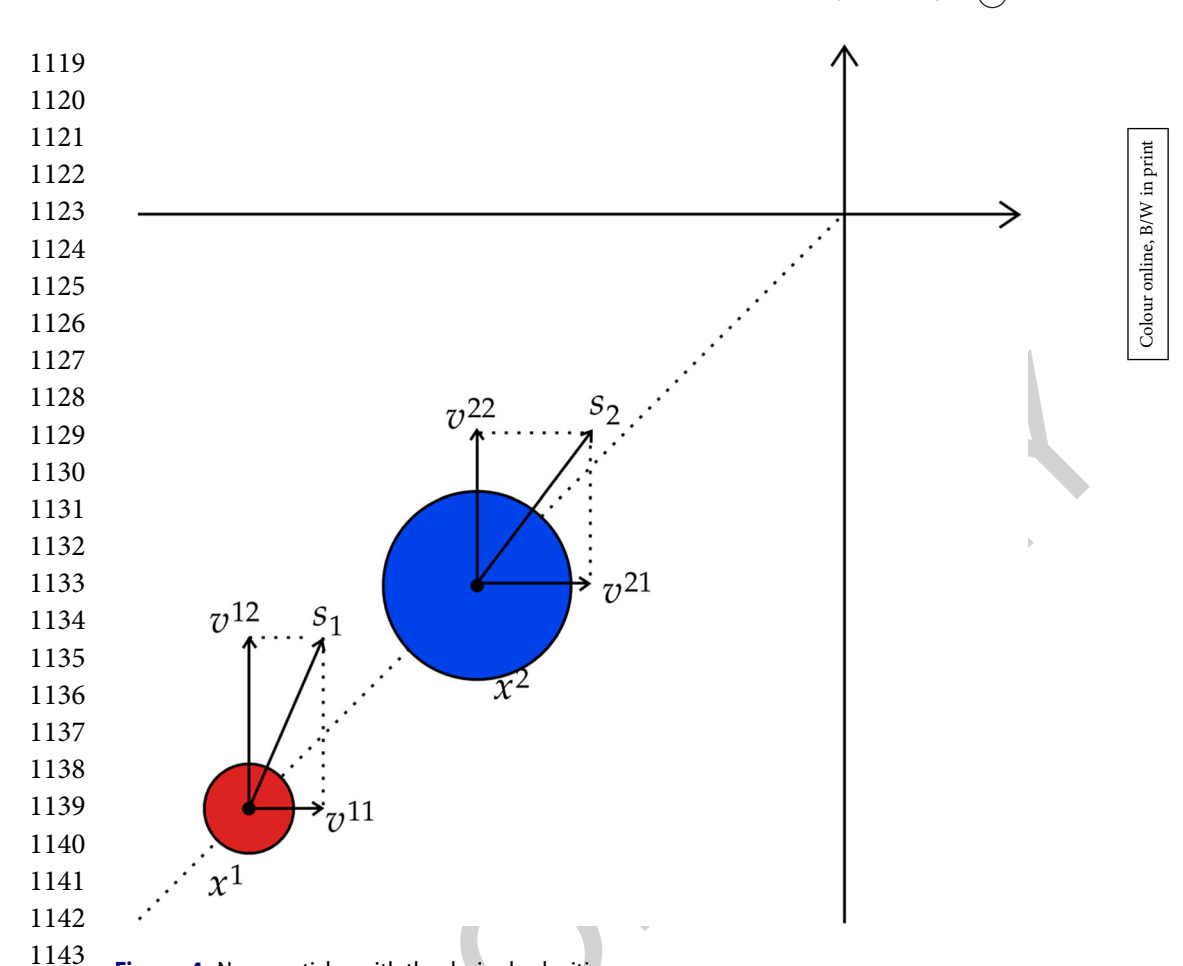


Figure 4. Nanoparticles with the desired velocities.

1144

1148 1149

1147

(1) $-(\dot{\bar{x}}^{11}(t), \dot{\bar{x}}^{12}(t), \dot{\bar{x}}^{21}(t), \dot{\bar{x}}^{22}(t)) = \eta(t)(1, 1, -1, -1) -$ 1150 $(s_1|\bar{u}^1(t)|\cos\theta^u, s_1|\bar{u}^1(t)|\sin\theta^u, s_2|\bar{u}^2(t)|\cos\theta^u, s_2|\bar{u}^2(t)|\sin\theta^u)$ for a.e. 1151 $t \in [0, \overline{T}].$ 1152

- (2) $\|\bar{x}^1(t) \bar{x}^2(t)\| > R_1 + R_2 \Longrightarrow \eta(t) = 0 \text{ for a.e. } t \in [0, \overline{T}].$ 1153
- (3) $\eta(t) > 0 \Longrightarrow \langle x_*, q(t) \rangle = 0$ for a.e. $t \in [0, \overline{T}]$. 1154
- (4) $(-p(\overline{T}) \eta(\overline{T})x_*, \overline{H}) \in \nabla \varphi(\overline{x}(\overline{T}), \overline{T}) \text{ where } \overline{H} := \frac{1}{\overline{T}} \in t_0^{\overline{T}} \langle p(t), \overline{x}(t) \rangle dt.$ 1155
- (5) $q(t) = p(t) \epsilon t_{(t,\overline{T})} d\gamma (\tau) x_*$ for all $t \in [0,\overline{T}]$ except at most a countable 1156 subset. 1157
- 1158 (6) $\langle \psi(t), \bar{u}(t) \rangle = \max_{u \in U} \langle \psi(t), u \rangle$, where $\psi(t) := \nabla_{u} g(\bar{x}(t), \bar{u}(t))^* q(t)$ for a.e. $t \in [0, \overline{T}]$. 1159
- (7) $\eta(\overline{T}) > 0 \Longrightarrow \|\bar{x}^1(\overline{T}) + \bar{x}^2(\overline{T})\| = R_1 + R_2.$ 1160
- (8) $\dot{p}(t) = 0$, for a.e. $t \in [0, \overline{T}]$ 1161

Taking into account that the nanoparticle directions are constant as well as the assumptions in the model imposed above, we seek for simplicity constant optimal controls. Then it follows from condition 2 that the function $\eta(\cdot)$ is piecewise constant on $[0, \overline{T}]$ and admits the representation

$$\eta(t) = \begin{cases}
0 & \text{for } t \in [0, t_*), \\
\eta & \text{for } t \in [t_*, \overline{T}].
\end{cases}$$
(35)

Using now 1, the dynamic equations prior to and after the time t_* can be rewritten

$$\begin{cases} \dot{\bar{x}}^{1}(t) = \left(s_{1}|\bar{u}^{1}|\cos\theta^{u}, s_{1}|\bar{u}^{1}|\sin\theta^{u}\right) & \text{and} \\ \dot{\bar{x}}^{2}(t) = \left(s_{2}|\bar{u}^{2}|\cos\theta^{u}, s_{2}|\bar{u}^{2}|\sin\theta^{u}\right) & \text{for } t \in [0, t_{*}), \end{cases}$$

$$\begin{cases} \dot{\bar{x}}^{1}(t) = \left(-\eta(t) + s_{1}|\bar{u}^{1}|\cos\theta^{u}, -\eta(t) + s_{1}|\bar{u}^{1}|\sin\theta^{u}\right) & \text{and} \\ \dot{\bar{x}}^{2}(t) = \left(\eta(t) + s_{2}|\bar{u}^{2}|\cos\theta^{u}, \eta(t) + s_{2}|\bar{u}^{2}|\sin\theta^{u}\right) & \text{for } t \in [t_{*}, \overline{T}]. \end{cases}$$

At the contacting time $t = t_*$, the two nanoparticles have the same velocities till the end of the straight tube, which yields $\dot{\bar{x}}^1(t) = \dot{\bar{x}}^2(t)$ for all $t \in [t_*, \overline{T}]$. This gives us in turn the following calculation of the corresponding value of η in representation (35):

$$\eta = \begin{cases} \frac{1}{2} \left(s_1 |\bar{u}^1| \cos \theta^u - s_2 |\bar{u}^2| \cos \theta^u \right) & \text{if } s_1 |\bar{u}^1| \neq s_2 |\bar{u}^2| \text{ and } \cos \theta^u = \sin \theta^u, \\ 0 & \text{otherwise} \end{cases}$$
(36)

The case of $\eta = 0$ is trivial. Applying the first formula in (36) and the constant nanoparticles velocity after the contacting time till reaching the target, we deduce from the Newton-Leibniz formula that

Note that $\|\bar{x}^2(t_*) - \bar{x}^1(t_*)\| = R_1 + R_2$ at the contacting time $t = t_*$. Recalling then that we use the sum norm yields the following equation for t_* :

$$|\bar{x}^{21}(0) - \bar{x}^{11}(0) + t_* \left(s_2 |\bar{u}^2| - s_1 |\bar{u}^1| \right) \cos \theta^u |$$

$$+ |\bar{x}^{22}(0) - \bar{x}^{12}(0) + t_* \left(s_2 |\bar{u}^2| - s_1 |\bar{u}^1| \right) \sin \theta^u | = R_1 + R_2, \quad (38)$$

which makes the connection between t_* and the control $\bar{u} = (\bar{u}^1, \bar{u}^2)$ via the given model data. Since the trajectory does not hit the boundary before $t = t_*$, we deduce from 4, 5, and 8 that

1209
1210
$$q(t) \equiv -\mu \bar{x}(\overline{T}) - (1, -1) \left(\eta(\overline{T}) + \gamma ([t, \overline{T}]) \right) =: (r_*^1, r_*^2) \in \mathbb{R}^4$$
 (39)

for all $t \in [0, t_*)$. Thus the maximization condition in **6** tells us that

$$\langle r_*^1, \bar{u}^1(t) \rangle + \langle r_*^2, \bar{u}^2(t) \rangle = \max_{u \in U} \left\{ \langle r_*^1, u^1 \rangle + \langle r_*^2, u^2 \rangle \right\}$$

for a.e. $t \in [0, t_*)$, which can be written by (39) as

1219
$$\langle -\mu \bar{x}^{1}(\overline{T}) - \mu \bar{x}^{2}(\overline{T}) + (\eta(\overline{T}) + \gamma([t, \overline{T}])), (-\bar{u}^{1}(t) + \bar{u}^{2}(t)) \rangle$$
1220
$$= \max_{u \in U} \left\{ \langle -\mu \left(\bar{x}^{1}(\overline{T}) + \bar{x}^{2}(\overline{T}) \right) + \left(\eta(\overline{T}) + \gamma([t, \overline{T}]) \right), (-u^{1} + u^{2}) \rangle \right\}$$
(40)

with $\eta(\overline{T}) \geq 0$. Considering the case when the optimal control controls \overline{u}^1 and \bar{u}^2 are interior points of the control domain U, we have from the maximization of the function

$$\phi(u^{1}, u^{2}) := \langle u^{1}, \left(-\eta(\overline{T}) - \gamma([t, \overline{T}]) - \mu \overline{x}^{1}(\overline{T}) \right) \rangle$$
$$+ \langle u^{2}, \left(\eta(\overline{T}) + \gamma([t, \overline{T}]) - \mu \overline{x}^{2}(\overline{T}) \right) \rangle$$

the following explicit conditions:

1233 • If
$$\|\bar{u}^1(t)\| < 3$$
, then $-\eta(\overline{T}) - \gamma([t, \overline{T}]) = \mu \bar{x}^1(\overline{T})$.
• If $\|\bar{u}^2(t)\| < 3$, then $\eta(\overline{T}) + \gamma([t, \overline{T}]) = \mu \bar{x}^2(\overline{T})$.

If both cases above occur, then we get $\mu(\bar{x}^1(\overline{T}) + \bar{x}^2(\overline{T})) = 0$. The last equation gives us the relationship

$$\bar{x}^1(\overline{T}) + \bar{x}^2(\overline{T}) = 0,$$

provided that $\mu = 1$ assumed without loss of generality. Combining the latter with (37) gives us $\overline{T}|\bar{u}^2| \approx 8.3275e - 13$. Furthermore, it follows from (38) that either $t_*|\bar{u}^2|\approx 6.1372e-13$, or $t_*|\bar{u}^2|\approx 6.7832e-13$. Examine now both these possibilities for t_* .

Case 1: If $t_*|\bar{u}^2|\approx 6.1372e-13$, then we get $\overline{T}\approx 1.3569t_*$. Furthermore, using (36) and the fminsearch program from MATLAB for the cost functional

1248 $J[\bar{x}, \bar{u}, \bar{T}]$, we obtain that

1265

1267

1268

1269

1282

1283

1284

1285

1286 1287

1288

1250
1251
1252

$$\eta = \frac{1}{2} \left(2s_1 |\bar{u}^2| \left(\frac{\sqrt{2}}{2} \right) - s_2 |\bar{u}^2| \left(\frac{\sqrt{2}}{2} \right) \right) = (1.1609e + 14) |\bar{u}^2| \neq 0$$
1252

1253 and that the following expressions hold:

1254
1255
1256
1257
1258
1259
1260
1261
1262

$$\bar{x}^{1}(t) \approx 2.3806, |\bar{u}^{2}| \approx 1.1903, \\ \bar{x}^{1}(t) \approx (-350 - (5.3126e + 14)t, -350 - (5.3126e + 14)t), \\ t \in [0, 5.1688e - 13), \\ \bar{x}^{1}(t) \approx (-278.5765 + (3.9308e + 14)t, -278.5765 + (3.9308e + 14)t), \\ t \in [5.1688e - 13, 7.0135e - 13], \\ \bar{x}^{2}(t) \approx (-200 - (2.5489e + 14)t, -200 - (2.5489e + 14)t), \\ t \in [0, 5.1688e - 13), \\ \bar{x}^{2}(t) \approx (-271.4235 + (3.9307e + 14)t, -271.4235 + (3.9307e + 14)t),$$

1263
$$\bar{x}^2(t) \approx (-271.4235 + (3.9307e + 14)t, -271.4235 + (3.9307e + 14)t$$

1264 $t \in [5.1688e - 13, 7.0135e - 13],$

1266 with
$$t_* = 5.1688e - 13$$
, $\overline{T} = 7.0135e - 13$, and $J = 14.3596$.

Case 2: If $t_*|\bar{u}^2| \approx 6.7832e - 13$, then we get $\overline{T} \approx 1.2277t_*$. Furthermore, using (36) and fminsearch program from MATLAB for the cost functional $J[\bar{x}, \bar{u}, \overline{T}]$, we obtain that

1270
1271
1272
$$|\bar{u}^{1}| \approx 2.3804, |\bar{u}^{2}| \approx 1.1902,$$
 $\bar{x}^{1}(t) \approx (-350 + (5.3122e + 14)t, -350 + (5.3122e + 14)t),$
1273
1274
1275
1276
1277
1278
 $\bar{x}^{1}(t) \approx (-271.5966 + (3.9305e + 14)t, -271.5966 + (3.9305e + 14)t),$
 $t \in [5.6744e - 13, 6.9665e - 13],$
 $\bar{x}^{2}(t) \approx (-200 + (2.5487e + 14)t, -200 + (2.5487e + 14)t),$
 $t \in [0, 5.6744e - 13),$
1279
1280
1281
 $\bar{x}^{2}(t) \approx (-278.4034 + (3.9304e + 14)t, -278.4034 + (3.9304e + 14)t),$
 $t \in [5.6744e - 13, 6.9665e - 13].$

Then the corresponding value of the cost functional is J = 36.3565.

Comparing the cost functional values in the two cases above, we confirm that $(\bar{u}^1, \bar{u}^2) = (5.3126e + 14, 5.3126e + 14, 3.9308e + 14, 3.9308e + 14)$ is the optimal control to this problem.

6. Concluding remarks

The paper presents applications of newly derived necessary optimality conditions for free-time optimal control of sweeping processes to practical problems arising in marine surface vehicle and nanoparticles models. This is done for the first time in the literature. The obtained results and calculations demonstrate the efficiency of the established optimality conditions to solve practical problems under certain assumptions that simplify the calculations. In our future research on these and related topics, we intend to relax the imposed assumptions to be able, in particular, to determine optimal strategies in these and related models among variable control actions in the corresponding sweeping processes.

1297 1298 1299

1300

1301

1302

1303

1304

1291 1292

1293 1294

1295

1296

Acknowledgments

The authors are gratefully indebted to Giovanni Colombo for his great contributions to our joint paper [36] and further discussions on the material presented in this paper. We are pleased to thank Messaoud Bounkhel, a former student of Lionel Thibault, for drawing our attention to his papers [7, 20] on the modelling and simulation in USV and nanoparticle systems. Our gratitude goes also to two anonymous referees and the handling editor whose remarks allowed us to improve the original presentation,

1305 1306 1307

1308

1310 1311

1312

1313

1314

1315

1316

1317

1321

1322

1323

1324

1325

1326

1327

1328

1329

1330

Disclosure statement

1309 No potential conflict of interest was reported by the author(s). O2

Funding

Boris S. Mordukhovich: Research of this author was partially supported by the USA National Science Foundation [grant numbers DMS-1007132 and DMS-1512846], by the Australian Research Council [discovery project DP-190100555], and by Project 111 of China [grant number D21024]. Dao Nguyen: Research of this author was supported by the AMS-Simon Foundation. Trang Nguyen: Research of this author was partially supported by the USA National Science Foundation [grant number DMS-1512846].

1318 1319

References 1320

Q3

- [1] Moreau JJ. On unilateral constraints, friction and plasticity. In: Capriz G, Stampacchia G, editors. New Variational Techniques in Mathematical Physics. Proc. C.I.M.E. Summer Schools, Cremonese, Rome; 1974. p. 173-322.
- [2] Adly S, Haddad T, Thibault L. Convex sweeping process in the framework of measure differential inclusions and evolution variational inequalities. Math Program. 2014;148:5-47. doi: 10.1007/s10107-014-0754-4
- [3] Bounkhel M. Mathematical modeling and numerical simulations of the motion of nanoparticles in straight tube. Adv Mech Eng. 2016;8:1-6. doi: 10.1177/168781401665 6965
- [4] Brogliato B, Tanwani A. Dynamical systems coupled with monotone set-valued operators: formalisms, applications, well-posedness, and stability. SIAM Rev. 2020;62:3-129. doi: 10.1137/18M1234795
- 1331 [5] Brokate M, Sprekels J. Hysteresis and phase transitions. New York: Springer; 1996.
- 1332 [6] Colombo G, Thibault L. Prox-regular sets and applications. In: Gao DY, Motreanu D, 1333 editors. Handbook of Nonconvex Analysis. Boston: International Press; 2010. p. 99-182.



- 1334 [7] Hedjar R, Bounkhel M. An automatic collision avoidance algorithm for multi-1335 ple marine surface vehicles. Int J Appl Math Comput Sci. 2019;29:759–768. doi: 1336 10.2478/amcs-2019-0056
- [8] Krasnosel'skii MA, Pokrovskii AV. Systems with hysteresis. New York: Springer; 1989.
- [9] Krečí P. Evolution variational inequalities and multidimensional hysteresis operators. In:
 Drabek P, Krečí P, Takac P, editors. Nonlinear Differential Equations. Res. Notes Math.
 Boca Raton, FL: Chapman & Hall/CRC; 1999; Vol. 404.
- 1340 [10] Maury B. A time-stepping scheme for inelastic collisions. Numer Math. 2006;102:649–1341 679. doi: 10.1007/s00211-005-0666-6
- 1342 [11] Monteiro Marques MDP. Differential inclusions in nonsmooth mechanical problems: shocks and dry friction. Basel: Birkhäuser; 1993.
- [12] Siddiqi AH, Manchanda P, Brokate M. On some recent developments concerning Moreau's sweeping process. In: Trends in Industrial and Applied Mathematics. Dordrecht, The Netherlands: Kluwer; 2002; Vol. 72. p. 339–354.
- 1346 [13] Thibault L. Sweeping process with regular and irregular sets. J Differ Equ. 2003;193:1–26. doi: 10.1016/S0022-0396(03)00129-3
- 1348 [14] Tolstonogov AA. Polyhedral sweeping processes with unbounded nonconvex-valued perturbation. J Differ Equ. 2020;63:7965–7983.
- [15] Venel J. A numerical scheme for a class of sweeping process. Numer Math. 2011;118:367–400. doi: 10.1007/s00211-010-0329-0
- 1351 [16] Edmond JF, Thibault L. Relaxation of an optimal control problem involving a perturbed sweeping process. Math Program. 2005;104:347–373. doi: 10.1007/s10107-005-0619-y
- [17] Thibault L. Unilateral variational analysis in Banach spaces. Singapore: World Scientific;
 2023. published in two volumes.
- 1355 [18] Adam L, Outrata JV. On optimal control of a sweeping process coupled with an ordinary differential equation. Discrete Contin Dyn Syst Ser B. 2014;19:2709–2738.
- 1356 [19] Arroud CE, Colombo G. A maximum principle for the controlled sweeping process.

 Set-Valued Var Anal. 2018;26:607–629. doi: 10.1007/s11228-017-0400-4
- 1358 [20] Brokate M, Krejčí P. Optimal control of ODE systems involving a rate independent variational inequality. Discrete Contin Dyn Syst Ser B. 2013;18:331–348.
- 1360 [21] Cao TH, Mordukhovich BS. Optimal control of a nonconvex perturbed sweeping process. J Differ Equ. 2019;266:1003–1050. doi: 10.1016/j.jde.2018.07.066
- [22] Cao TH, Mordukhovich BS. Applications of optimal control of a nonconvex sweeping process to optimization of the planar crowd motion model. Discrete Contin Dyn Syst Ser B. 2019;24:4191–4216.
- 1364 [23] Colombo G, Henrion R, Hoang ND, et al. Optimal control of the sweeping process. Dyn Contin Discrete Impuls Syst Ser B. 2012;19:117–159.
- 1366 [24] Colombo G, Henrion R, Hoang ND, et al. Optimal control of the sweeping process over polyhedral controlled sets. J Differ Equ. 2016;260:3397–3447. doi: 10.1016/j.jde.2015.10.039
- 1368 [25] Colombo G, Mordukhovich BS, Nguyen D. Optimal control of sweeping processes in robotics and traffic flow models. J Optim Theory Appl. 2019;182:439–472. doi: 10.1007/s10957-019-01521-y
- 1371 [26] Colombo G, Mordukhovich BS, Nguyen D. Optimization of a perturbed sweeping process by discontinuous controls. SIAM J Control Optim. 2020;58:2678–2709. doi: 10.1137/18M1207120
- [27] de Pinho Md.R, Ferreira MMA, Smirnov GV. Optimal control involving sweeping processes. Set-Valued Var Anal. 2019;27:523–548. doi: 10.1007/s11228-018-0501-8
- 1375 [28] de Pinho Md.R, Ferreira MMA, Smirnov GV. A maximum principle for optimal control problems involving sweeping processes with a nonsmooth set. J Optim Theory Appl. 2023;199:273–297. doi: 10.1007/s10957-023-02283-4



- 1377 [29] Henrion R, Jourani A, Mordukhovich BS. Controlled polyhedral sweeping processes: 1378 existence, stability, and optimality condition. J Differ Equ. 2023;366:408–443. doi: 10.1016/j.jde.2023.04.010
- 1380 [30] Hermosilla C, Palladino M. Optimal control of the sweeping process with a nonsmooth moving set. SIAM J Control Optim. 2022;60:2811–2834. doi: 10.1137/21M1405472
- 1381 [31] Nour C, Zeidan V. Pontryagin-type maximum principle for a controlled sweeping process with nonsmooth and unbounded sweeping set. J Convex Anal. 2024;31:1.
- 1383 [32] Zeidan V, Nour C, Saoud H. A nonsmooth maximum principle for a controlled nonconvex sweeping process. J Differ Equ. 2020;269:9531–9582. doi: 10.1016/j.jde.2020.06.053
- 1385 [33] Clarke F. Functional analysis, calculus of variations and optimal control. London:
 Springer; 2013.
- 1387 [34] Mordukhovich BS. Variational analysis and generalized differentiation, II: applications. Berlin: Springer; 2006.
- 1388 [35] Vinter RB. Optimal control. Boston: Birkhaüser; 2000.
- [36] Colombo G, Mordukhovich BS, Nguyen D, et al. Discrete approximations and optimality
 conditions for controlled free-time sweeping processes. Appl Math Optim. 2024;89:40.
 doi: 10.1007/s00245-024-10108-7
- 1392 [37] Mordukhovich BS. Discrete approximations and refined Euler-Lagrange conditions for differential inclusions. SIAM J Control Optim. 1995;33:882–915. doi: 10.1137/S0363012993245665
- 1394 [38] Cao TH, Colombo G, Mordukhovich BS, et al. Optimization and discrete approxima-1395 tion of sweeping processes with controlled moving sets and perturbations. J Differ Equ. 1396 2021;274:461–509. doi: 10.1016/j.jde.2020.10.017
- 1397 [39] Cao TH, Mordukhovich BS. Optimality conditions for a controlled sweeping process with applications to the crowd motion model. Discrete Contin Dyn Syst Ser B. 2017;21:267–306.
- 1399 [40] Colombo G, Gidoni P. On the optimal control of rate-independent soft crawlers. J Math Pures Appl. 2021;146:127–157. doi: 10.1016/j.matpur.2020.11.005
- 1401 [41] Mordukhovich BS, Nguyen D. Discrete approximations and optimal control of nonsmooth perturbed sweeping processes. Convex Anal. 2021;28:655–688.
- 1403 [42] Mordukhovich BS. Variational analysis and generalized differentiation, I: basic theory.

 Berlin: Springer; 2006.
- [43] Mordukhovich BS. Variational analysis and applications. Cham, Switzerland: Springer; 2018.
- 1406 [44] Rockafellar RT, Wets RJ-B. Variational analysis. Berlin: Springer; 1998.
- 1407 [45] Mordukhovich BS. Second-order variational analysis in optimization, variational stabil-1408 ity, and control: theory, algorithms, applications, to appear in Springer, 2024.
- 1409 [46] Skjetne R, Fossen TI, Kokotovic PV. Adaptive maneuvering, with experiments, for a model ship in marine control laboratory. Automatica. 2005;41:289–298. doi: 10.1016/j.automatica.2004.10.006
- 1411 Zhao Y, Skalak R, Chien S. Hydrodynamics in cell rolling and adhesion. In: Simon B, editor. Advances in bioengineering. New York: American Society of Mechanical Engineers; 1997. p. 79–80.
- 1414 [48] Zhao Y, Chien S, Weinbaum S. Dynamic contact forces on leukocyte microvilli and their penetration of the endothelial glycocalyx. Biophys J. 2001;80:1124–1140. doi: 10.1016/S0006-3495(01)76090-0
- [49] Sakariassen KS, Orning L, Turitto VT. The impact of blood shear rate on arterial thrombus formation. Future Sci OA. 2015;1:FSO30. doi: 10.4155/fso.15.28